

國立交通大學

電機學院光電顯示科技產業研發碩士班

碩 士 論 文

表面能調整於定義有機薄膜電晶體主動區
之應用

**Pentacene patterning by the adjustment of
surface energy and its application in OTFTs**

研究生：邱育敏

指導教授：冉曉雯 博士

中華民國 九十六年 二月

表面能調整於定義有機薄膜電晶體主動區之應用

Pentacene patterning by the adjustment of surface energy and
its application in OTFTs

研究生：邱育敏

Student：Yu-Min Chiou

指導教授：冉曉雯 博士

Advisor：Dr. Hsiao-Wen Zan

國立交通大學

電機學院光電顯示科技產業研發碩士班



Submitted to College of Electrical and Computer Engineering

National Chiao Tung University

in partial Fulfillment of the Requirements

for the Degree of

Master

in

Industrial Technology R & D Master Program on

Photonics and Display Technologies

February 2007

Hsinchu, Taiwan, Republic of China

中華民國九十六年二月

表面能調整於定義有機薄膜電晶體主動區之應用

研究生:邱育敏

指導教授:冉曉雯 博士

國立交通大學電機學院產業研發碩士班

摘 要

在此論文中，我們藉由表面能調整，已成功定義出五環素有機薄膜電晶體(pentacene based-OTFTs)的主動區域。首先，利用自組裝單層膜(SAM)來作介電層的表面處理，並透過石英光罩照射 UV 光等方法，來加以控制所需區域的表面能。接著，在處理過的介電層表面沉積上 pentacene 薄膜後，只需經由簡易的去離子水浸洗過程，便能將照射過 UV 光部分的 pentacene 薄膜移除，而獲得所要的主動層區域。另外，藉由吸附能與侵入能的分析，我們可知此方法為一剝除機制，而介於 pentacene 薄膜、基板與去離子水間的不同侵入能，便是成功定義出主動區的關鍵因素。而我們所提出的此定義方式，亦可與傳統的黃光微影製程結合，製作出 OTFTs 陣列。

接著，我們將浸洗後獲得的 pentacene 區域製作成元件來驗證此方法的可行性。藉由元件特性的分析，我們觀察到其可靠度等特性依然優於傳統結構的對照元件，載子移動率、電流開/關比值(大於 10^6)以及次臨界擺幅等特性皆有明顯的改善。

Pentacene patterning by the adjustment of surface energy and its application in OTFTs

Student: Yu-Min Chiou

Advisor: Dr. Hsiao-Wen Zan

Institute of Electro-Optical Engineering

National Chiao Tung University

Abstract

In this thesis, the pentacene patterning by adjusting the surface energy was discussed. Firstly the surface energy was controlled by the self-assembled layer (SAM) treatment and the partial ultra-violet (UV) light exposure through quartz-glass mask. Then, after pentacene deposition, water dipping was used to remove the pentacene on UV-exposed area. The adhesion energy and the intrusion energy were analyzed to reveal that the dipping was a lift-off process and the key for successful patterning was the intrusion energy between pentacene, substrate (hydrophilic or hydrophobic) and the D.I. water. The proposed technology was compatible to conventional lithography system and is applicable to OTFT arrays.

Next, the remaining pentacene film was fabricated as a top-contact OTFTs to confirm the practicability of this technology. According to the output characteristics of OTFTs, the

performance kept favorable and superior to that of the control sample. The mobility, the on/off current ratio (higher than 10^6) and the sub-threshold swing were also improved.



誌謝

時光飛逝，又到了畢業的時刻。在交大顯示所的兩年碩士生涯，讓我成長很多。首先，要感謝我的指導教授冉曉雯老師，老師不僅對我研究上悉心指導，在人生的態度上，也適時地給了我許多不錯的建議，亦師亦友，親切又不失威嚴的教導方式，讓我在這兩年的學習過程既充實又開心。

接著，要感謝國錫、政偉、士欽學長們不厭其煩的指出我研究中的缺失，且在我有研究上的問題時，願意仔細詳盡的為我解答。還有謝謝已畢業的學長姐：傑斌、溥寬、庭軒、貞儀、章祐、全生，讓我在懵懂時能對 TFT 有基礎的知識。也感謝志宏同學平日的幫忙，以及好友子怡的陪伴談心，真的很高興能有妳如此窩心的朋友，雖然妳已在遙遠的地方，但我滿滿的祝福仍將傳達給妳，相信妳這愛漂亮的小子，也必定是那天堂最美麗的天使，與妳的這段回憶，會永留我心中…我的摯友！

而最要感謝的就是常和我一起熬夜作 run 的睿志、廷遠、德倫以及皇維，有你們幾個小鬼的相伴及搞笑，使得沉悶的研究生活增添了許多歡樂，也相信我們未來仍將會是常聯絡的好友。另外還要感謝而康、光明、文馨、芸嘉、學弟們及和我一同修習教育學程的外所朋友，你們讓我有機會對不同面向的研究也能有更廣泛的認識，也謝謝你們平常的關心。

最後要感謝我的父母、家人及我最要好的朋友，感謝你們一路對我的支持與照顧，使我的研究過程變的更溫馨而甘甜。

謝謝大家，有你們的相伴，讓我有快樂又難忘的每一天！

於交大交映 501

2007.02.09

Contents

Chinese Abstract	I
English Abstract	II
Acknowledgement	IV
Contents	V
Table Captions	VII
Figure Captions	VIII
Chapter 1. Introduction	1
1-1 Introduction of Organic Thin Film Transistors (OTFTs)	1
1-2 Organic semiconducting materials	4
1-3 Surface treatment	8
1-4 Operating mode of OTFTs	9
1-5 Motivation	11
1-6 Thesis Organization	12
Chapter 2. Device structures, fabrication and parameters extraction	13
2.1 Device structures and fabrication	13
2.1-1 OTFTs with differential surface energy	13
2.1-2 OTFTs with patterned pentacene	15
2.2 Methods of Device parameters extraction	18
2.2-1 Mobility	18
2.2-2 Threshold voltage	19
2.2-3 On/Off current ratio	19
2.2-4 Subthreshold swing	19
2.2-5 Surface free energy	20
Chapter 3. Result and Discussion	21
3.1 Self-Assembly Monolayer (SAM)	21
3.2 Surface energy control	22
3.3 Pentacene patterning	25
Chapter 4. Conclusion	28

References	29
Tables	35
Figures	38
Profile	55



Table Captions

Chapter 1

Table I Comparisons of TFTs using different materials

Chapter 3

Table II Contact angle, Surface energies and Surface roughnesses of SiO₂ treated by different ODMS concentrations.

Table III Comparison of the transfer characteristics of OTFTs under different UV-exposed time

Table IV Comparison of the transfer characteristics of OTFTs under different conditions.



Figure Captions

Chapter 1

Fig. 1.1 Molecular structure of (a) sexithiophene and (b) pentacene.

Fig. 1.2 Mobility of the organic semiconductors has been improved by five orders of magnitude over the past 15 years.

Fig. 1.3 Prominent (a) p-type and (b) n-type organic semiconductor materials.

Fig. 1.4 Semilogarithmic plot of mobility vs. year

Fig. 1.5 Energy band diagram of pentacene.

Fig. 1.6 Chemical structure of ODMS – SAMs.

Fig. 1.7 OTFT device configurations. (a) Schematic cross section view of top contact device. (b) Schematic cross section view of bottom contact device.

Fig. 1.8 Schematic of operation of OTFT, showing a p-type semiconductor: + indicates a positive charge in semiconductor; - indicate a negatively charge. (a) no-bias (b) accumulation mode (c) depletion mode.

Fig. 1.9 Energy band diagrams for (a) a p-channel (pentacene) and for (b) a n-channel (NTCDA) OTFTs under different gate bias conditions.

Chapter 2

Fig. 2.1 The ODMS layer changed the gate dielectric surface from hydrophilic to hydrophobic.

Fig. 2.2 Process flow of ODMS treatment and the ultra-violet (UV) light exposure

Fig. 2.3 (a) conventional OTFTs and (b) OTFTs with ODMS treatment and with different UV exposure times.

Fig.2.4 The gate dielectric surface was partial exposed to UV light through

quartz-glass mask.

Fig. 2.5 The lift-off process for pentacene patterning.

Chapter 3

Fig. 3.1 Comparison of dielectric (a) contact angle and (b) surface energy when treated by ODMS in different solvents.

Fig. 3.2 (a) The water contact angle and (b) the surface energy as a function of ODMS concentration. Solvents as alcohol and toluene are compared.

Fig. 3.3 (a) Contact angle and (b) surface energy of SiO₂ treated by different concentrations of ODMS .Alcohol was used as solvent.

Fig. 3.4 (a) The water contact angle on ODMS-treated SiO₂ surface as a function of UV exposure time. (b) The extracted surface energy and its polar and dispersion components were shown as a function of UV exposure time.

Fig. 3.5 (a) The transfer I_D – V_G curves of various OTFTs with conditions described in Table III and Fig. 2.3 (b) The output I_D-V_D curves of ODMS treatment device.

Fig. 3.6 (a) The AFM images of the pentacene deposited on non-UV-exposed region and on 30-mins UV-exposed region. (b) The AFM image and the step profile of patterned pentacene film.

Fig. 3.7 The variation of E_A (adhesion energy before dipping) , E_I (intrusion energy) , and E_A' (adhesion energy after dipping) as a function of UV exposure time.

Fig. 3.8 (a) The transfer I_D – V_G curves of various OTFTs with conditions described in Table IV. (b) The output I_D-V_D curves of OTFTs with patterned pentacene.

Chapter 1

Introduction

1.1 Introduction of Organic Thin Film Transistors (OTFTs)

Organic semiconductors have been known since the late 1940s [1]. After Shirakawa began the research on the conducting property of polymers in late 1970s [2]. However, apart from a very small number of preliminary works on conjugated small molecules [3,4] and polymers[5], the concept of using organic materials as semiconductors layer in transistors are realized at least since the 1980s [6,7]. Then, the first transistor based on an organic semiconductor was only reported in 1986,[8,9] with a device made on an electrochemically grown polythiophene film. But the mobility was quite low, on the order of $10^{-5}\text{cm}^2/\text{Vs}$. The conductivity of the polymer can be altered from insulator to conductor through the method of doping. Polythiophene belongs to the family of the conducting polymers that were discovered in the late 1970s.[10] The inventors of polyacetylene, an archetypal model of conducting polymers, were awarded the Nobel Prize in chemistry in 2000. The possibility of fabricating organic TFT (OTFT) with small conjugated molecules was shown in 1989[11] with sexithiophene, an oligomer of polythiophene made of six thiophene rings linked at alpha position (see Fig. 1.1), showed mobility on the order of $10^{-1}\text{cm}^2/\text{Vs}$, which has reached the display-requirement and is comparable to the amorphous-Si TFTs. The comparisons

between amorphous-Si TFTs, poly-Si TFTs and OTFTs are listed in Table 1.1 [12].

Interestingly enough, the organic TFT grew in parallel with another device, the organic light-emitting diode (OLED). As in the case of OTFTs, OLEDs can be made with small molecules [13] or polymers [14]. However, the development of OLEDs has been much faster than that of OTFTs, so that commercial products based on OLEDs are now available on the market, which is not yet the case for OTFTs. Nowadays, a large number of conjugated molecules and polymers have been used to be the active layers of OTFTs. The most significant difference between distinguishing those devices fabrication is the deposition method. Organic semiconductors are potentially solvable in organic solvent and are compatible to deposit at low-temperature on plastic substrates. By the low-cost fabrication techniques such as spin-coating and inkjet-printing, OTFTs may be used in the applications of flexibility, large-area coverage without complex process system and saving more energy on green earth.

Since organic semiconductors can be processed at low temperatures and compatible with plastic substrates. Such applications include active-matrix liquid crystal displays (AMLCDs), active-matrix organic light-emitting diodes (AMOLEDs), and electronic paper displays. Additionally, organic sensors, organic solar cells, low-end smart cards, radio-frequency identification (RFID) tags, and other electronics integrated with organic circuits have been proposed. However, in spite of considerable improvements during the last

years, the performance of OTFTs remains far beyond that of their inorganic counterpart, except for a-Si:H. For this reason, applications are envisioned where low fabrication costs and large area are of primary importance. These include electronic bar codes and identification tags, and, to a lesser extent, active matrix elements for organic flat panel displays. With this in mind, more and more industrial groups have recently initiated research programs in the field of organic transistors. Until recently, much of the research effort has been directed at improving the charge-carrier mobility. Several papers have reviewed this search for better materials and device architecture[15-19].

In Fig. 1.2 [20], we can compare the increase of mobility in the past years for different organic semiconductors. If we want to overcome the materials limitation, there are several points we have to overcome. First, the injection from the contact electrodes to organic film must be optimized. Second, deposition conditions should be optimized to get the best molecular ordering. And third, the synthesis-technology will provide more opportunities for choosing new organic semiconductor. As shown in Fig. 1.3[21], the current topics on OTFTs are still focused on p-type semiconductors, the development of n-type semiconductors is expected and under investigation. The reliability and reproducibility are also important issues. There is still room for further improvement, and the choices of materials for the electrodes [22], the insulator [23], the passivations [24], and the substrates [25] are also important factor.

Recently, the organic thin film transistors (OTFTs) are of interest for the fabrication of low-cost, large-area, flexible displays and low-end electronics. The OTFTs performance has been improved in the past decade and comparable to the hydrogenated amorphous silicon transistors (a-Si:H TFT) [26]. To fabricate organic transistors on glass or flexible substrate, it is essential to lower down the process temperature. Many researchers have proposed individual methods to fabricate the pentacene-transistors and the reported field-effect mobilities are in the range of $10^{-3} \sim 3\text{cm}^2/\text{V}\cdot\text{sec}$ [27]. However, the OTFTs still face several problems: low-mobility, low-temperature gate dielectrics, and reliably large area processes, etc.

1.2 Organic semiconducting materials

Organic materials such as polythiophene, α -sexithiophene (α -6T) have been investigated for use in field effect transistors (FETs) [28]. Polycrystalline molecular solids such as α -sexithiophene (α -6T) or amorphous/semi-crystalline polymers such as polythiophene or acenes such as pentacene, teracene show the highest mobility [29]. Figure 1.4 shows the evolution of organic materials and the improvement in their mobility over the years [30]. Pentacene based FETs show the high mobility and have been extensively studied. Pentacene is made up of five benzene rings as shown in Fig. 1.1 Pentacene has a sublimation temperature of 300°C . Well ordered pentacene films can be deposited at low temperatures making it suitable for deposition on plastic substrates.

Organic conjugated materials used in OTFTs can be generally divided into two groups. Among the semiconductors, one group is the polymers and the other is the oligomers. The polymers are formed by a repeating chain of hydrogen and carbon in various configurations with other elements, but they have relatively poor mobilities ($4 \times 10^{-2} \text{ cm}^2/\text{Vs}$ [31]). The oligomers are held together by weak Van der Waal forces and thermal-evaporated with good ordering. Devices fabricated with oligomers have higher mobilities ($1.5 \text{ cm}^2/\text{Vs}$ [32]). The organic materials can function either as p-type or n-type. In p-type semiconductors, the majority carriers are holes; while in n-type the majority carriers are electrons. Among, p-type semiconductors are the most widely studied organic semiconductors. Recently, many molecular semiconductors, such as pentacene, thiophene oligomers, and regioregular poly(3-alkyl-thiophene) are proposed. The pentacene ($\text{C}_{22}\text{H}_{14}$) is a promising candidate for future electronic devices and an interesting model system, due to its superior field effect mobility and environmental stability [33].

Pentacene is one of the popular materials in OTFTs. Its mobility has reached the fundamental limit ($>3 \text{ cm}^2/\text{Vs}$) [34, 35] which is obtained with a single crystalline at room temperature. The mobility of pentacene is comparable to that of amorphous silicon which is widely developed and used in active matrix liquid crystal displays (AMLCD) and the other electronic applications.

Pentacene is an aromatic compound with five condensed benzene rings and therefore,

the chemical formula is $C_{22}H_{14}$ with molecular weight 278.3. The volume of the unit cell is about 705\AA [34]. The permittivity is 4 [35], and the electron affinity is about 2.49eV. Silinish *et al.* determined the adiabatic energy gap (E_G^{Ad}) by using the threshold function of intrinsic photoconductivity in pentacene [22]. The second transition is from the excited state to the ionic state, which is called the optical energy gap (E_G^{Opt}). According to Fig. 1.5, the adiabatic energy gap as 2.47eV and the optical energy gap as 2.83eV is recorded [36]. Pentacene is used as an active layer. Its purity leads to longer diffusion length for the charge transporting with less interaction with the lattice. Furthermore, the impurities in the material tend to chemically combine with the organic semiconductor material which leads to irregularities in the band gap [37]. Therefore, the thermal evaporation is carried out under high or ultra high vacuum conditions to avoid the impurities and increase the quality of the material. It is well known that the deposition temperature, deposition pressure, and deposition rate are the three critical parameters to the organic film quality. Lower deposition rate and appropriate deposition temperature is expected to result in better ordering of the organic molecules, thin-film phase formation of pentacene film, and the better performance [38]. In OTFTs, the roughness has a influence on the morphology, whereas the films on the smooth thermal oxide are in generally highly ordered. The surface chemistry also is a typical issue to organic devices. Changing surface wettability as a hydrophobic surface by surface treatment leads to mobilities increasing [39].

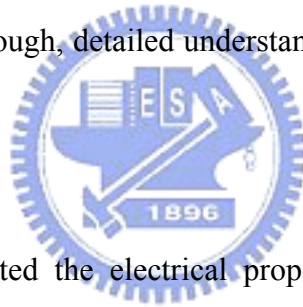
Carrier transportation in the organic semiconductors have been investigated on the theory and modeling in the past years [40]. Recently, two principal types of theoretical model are used to describe the transport in organic semiconductors : “The band-transport model” and “The hopping models”. However, band transport may not suit for some disordered organic semiconductors, in which carrier transport is govern by the hopping between localized states. Hopping is assisted by phonons and the mobility increases with temperature. Typically, the mobility is very low, usually much lower than $1\text{cm}^2/\text{V}\cdot\text{sec}$. The boundary between “band transport” and “hopping” is divided by materials mobilities ($\sim 1\text{cm}^2/\text{V}\cdot\text{sec}$) at room-temperature (RT) [41]. Many kinds of polycrystalline organic semiconductors , such as several members of the acene series including pentacene, rubrene, have RT mobility over the boundary [42]. Sometimes, temperature-independent mobility was found in some polycrystalline pentacene devices [43]. Thus, this observation argued that the simply thermal activated hopping process governed the whole carrier transport behaviors in high quality polycrystalline pentacene film, despite that the temperature independent mobility has been observed in exceptional cases [43].

Finally, the exact nature of the charge carrier transport in organic molecular crystals is still not well-understood, which has been the focus in many theoretical studies [44].

1.3 Surface treatment

Several researchers had verified the hydrophobic surface was more suitable for organic film deposition [45]. Since the hydrophobic polymer dielectric has lower or similar surface energy to organic films. The similar concept was also realized by self-assembled monolayer (SAM) on inorganic dielectrics. If the inorganic dielectrics with lower surface-energy, that may provide better performance and resulted in lower interface traps in OTFTs [46]. The surface properties such as frictional or abrasion, permeability, insulating properties, wettability and chemical reactivity are strongly dependent on a molecular aggregation state of the surface [47,48]. Therefore, the control of a molecular aggregation state on the film is important to construct a highly functionalized surface. One of the most effective ways of studying surface properties is contact angle measurement. The contact angle is the angle between the tangent to the drop's profile and the tangent to the surface at the intersection of the vapor, the liquid, and the solid. The contact angle is an index of the wettability of the solid surface. A low contact angle between solid surface water-drop indicates that the surface is hydrophilic and has a high surface energy. On the contrary, a high contact angle means that the surface is hydrophobic and has a low surface energy. The surface free energy was traditionally quantified by contact angle measurements [49,50].

Several investigations on the self-assembly monolayer (SAM) have been performed to elucidate the device structure, formation and performance [51, 52]. An SAM layer can change the gate dielectric surface from hydrophilic to hydrophobic. The organic film grown on a hydrophobic surface showed better adhesion [53], so the difference between the hydrophilic and hydrophobic properties can be exploited as an important factor for patterning the organic film [54]. A simple means of controlling the surface polarity (hydrophilic or hydrophobic) by using SAM layer and UV light exposure had been proposed [55, 56]. Selectively-ordered organic film deposited on the patterned SAM was demonstrated by Masahiko Ando *et. al* [55]. Though, detailed understanding of the variation of surface energy had not been discussed.



In this study, we fabricated the electrical properties of the OTFTs using pentacene fabricated by thermal evaporation in high vacuum with the one kinds of dielectric surface treatment material - ODMS (see Fig. 1.6).

1.4 Operation of OTFTs

A thin film transistor is composed of three basic elements: (i) a thin semiconductor film; (ii) an insulating layer; and (iii) three electrodes. Two of them, the source and the drain, are in contact with the semiconductor film at a short distance from one another. The third electrode, the gate, is separated from the semiconductor film by the insulating layer. Figure 1.7 show two kinds of standard OTFT device configurations, (a) is the top-contact device and (b) is the bottom-contact device, respectively. Actually, the general operation concepts are originated

from MOSFET theory. In traditional MOSFET, most devices are operated in inversion mode. However, the operation of OTFTs is generally in accumulation mode [57]. In Fig. 1.8 presents the schematic operation of OTFTs, showing a p-type semiconductor; + indicates a positive charge; - indicates a negative charge. When zero bias was applied to OTFTs, the schematic diagram is shown in Fig. 1.8(a). When a bias, V_G , is applied to the gate electrode shown in Fig. 1.8 (b), (c), the voltage-drop over the insulator and the semiconductor accumulates charges near the insulator/semiconductor interfaces. The typical I-V characteristics can be used to calculate the important parameters such as mobility, threshold voltage, and on/off current ratio.

Since the pentacene is a p-type semiconductor. Thus, negative bias is applied to the gate, the voltage-drop between insulator and semiconductor cause the band bending in the organic semiconductor. The additional positive charges will accumulate between the interfaces. The energy band diagrams for p-type and n-type OTFT are shown in Fig. 1.9. The insulator serves as a capacitance per unit area which stores charges and can be represented as C_{OX} , then the accumulated charge per unit area is about $V_G C_i$. Additionally, assuming that a negligibly small voltage, V_{th} , is dropped across the semiconductor. In this situation, the applied drain bias can drive the current from source to drain. The conduction is determined by the mobility (μ) which represents the driving ability of the electrical field on the accumulated charges. Therefore, the increased gate voltage δV_G accounts for the increased charges $C_{OX} \delta V_G$ and the total charges accumulated over the channel region are $WLC_{OX} \delta V_G$, where W and L corresponds to the channel width and length, respectively. If the increment of charge has a mobility: μ , and a small drain bias: V_D is applied then an incremental current δI_D is represented as

$$\delta I_D \approx \frac{W}{L} \mu C_{OX} V_D \delta V_G \quad (1.1)$$

In general, we can divide the operation of OTFTs into two regions, linear and saturation

regions. The drain current in the linear region is determined from the following equation:

$$I_D = \frac{W}{L} C_{OX} \mu (V_G - V_{TH} - \frac{V_D}{2}) V_D \quad (1.2)$$

Since the drain voltage is quite small, sometimes equation (1.2) can be simplified as

$$I_D = \frac{W}{L} C_{OX} \mu (V_G - V_{TH}) V_D \quad (1.3)$$

For $-V_D > -(V_G - V_{TH})$, I_D tends to saturate due to the pinch-off of the accumulation layer. The current equation is modified as:

$$I_D = \frac{W}{2L} C_{OX} \mu (V_G - V_{TH})^2 \quad (1.4)$$

The energy band diagrams for p-type and n-type OTFT are shown in Fig. 1.5. [58]

1.5 Motivation

Pentacene-based OTFT also suffer from large leakage current due to the difficulty of thin film patterning. Traditional lithography process is not applicable on pentacene thin film because the organic film will be damaged while the photo resist is removed. Currently shadow mask is used to define the pentacene pattern, the large resolution limits the scaling down of pentacene thin film. Since the deposition of pentacene can be greatly influenced by the surface condition, the self-aligned patterning technique had been proposed by using OTS SAM and oxygen plasma on PVP organic dielectric layer [59]. In this study, we also proposed a novel patterning technology. By introducing new SAM material (ODMS) onto SiO₂ dielectric film, the contact angle can be modified from 90 degree to 0 degree by UV light exposure. Since the pentacene molecules tend to grow on a hydrophobic surface, pentacene patterning can be achieved easily by pattern the UV light exposure area.

1.6 Thesis Organization

In Chapter 1, we described the introduction of OTFTs, development, brief overview and motivation of the thesis. In Chapter 2, the devices fabrication, measurement and parameter extraction of OTFTs are presented. In Chapter 3, different structures are investigated and discussed. Finally, we describe the conclusion and future work in Chapter 4.



Chapter 2

Device structures, fabrication and parameters extraction

2.1 Device structures and fabrication

2.1-1 OTFTs with differential surface energy

The devices used in this series of experiments are the top contact (TC) structure, which means the organic semiconductor layer is deposited on the bottom of the contact electrodes.

The detail fabrication processes are following:

Step1. Substrate and gate electrode

4-inch n-type heavily-doped single crystal silicon wafer with (100) orientation is used as substrate and gate electrode.



Step2. Gate oxide formation

After the initial RCA cleaning, the 1000Å thermally grown SiO₂ layer is deposited in furnace.

Step3. Surface treatment

The silicon oxide was treated by SAM - ODMS to let the surface of the silicon oxide be a hydrophobic one.

Step4. UV light exposure

As illustrated in Fig. 2.1, 2.2, the dielectric surface treated with SAM was exposed by UV light through various exposing condition. The contact angle and surface free energy was controlled by the exposing time of the UV-light.

Step5. Pentacene film deposition through shadow mask

The pentacene material obtained from Aldrich without any purification was directly placed in the thermal coater for the deposition. It is well known that the deposition pressure, deposition rate, and deposition temperature are the three critical parameters to the quality of the organic film [60]. The deposition is started at the pressure around 1×10^{-6} torr. The deposition rate is controlled at $\sim 0.5 \text{ \AA}/\text{sec}$ and the thickness of pentacene film was about 1000 \AA , monitored by the quartz crystal oscillator. Slower deposition rate is expected to result in smoother and better ordering of the organic molecules. The deposition temperature is also a factor influencing the pentacene film formation. The temperature we use in depositing pentacene films is $70 \text{ }^\circ\text{C}$. We use shadow mask to define the active region of each device.

Step6. Source/Drain deposition through the shadow mask

The injection barrier of the OTFT device is determined by the materials of the source and drain electrodes. Materials with large work function are preferred to form Ohmic contact [61]. The Au with work function $\sim 5.1 \text{ eV}$ does help to provide a better injection. Then, we

deposited Au as the source/drain electrodes on the pentacene film. The thickness of the electrode pad is 1000Å.

2.1-2 OTFTs with patterned pentacene

The devices used in this series of experiments are the top contact (TC) structure, which means the organic semiconductor layer is deposited on the bottom of the contact electrodes. The detail fabrication processes are following:

Step1. Substrate and gate electrode

4-inch n-type heavily-doped single crystal silicon wafer with (100) orientation is used as substrate and gate electrode.



Step2. Gate oxide formation

After the initial RCA cleaning, the 1000Å thermally grown SiO₂ layer is deposited in furnace.

Step3. Surface treatment

The silicon oxide was treated by SAM - ODMS to let the surface of the silicon oxide be a hydrophobic one.

Step4. UV light exposure through quartz-glass mask

As illustrated in Fig. 2.3, the surface was partial exposed by UV light through quartz-glass mask. The contact angle and surface free energy was controlled by the exposing time of the UV-light.

Step5. Pentacene film deposition

The pentacene material obtained from Aldrich without any purification was directly placed in the thermal coater for the deposition. It is well known that the deposition pressure, deposition rate, and deposition temperature are the three critical parameters to the quality of the organic film [60]. The deposition is started at the pressure around 1×10^{-6} torr. The deposition rate is controlled at $\sim 0.5 \text{ \AA}/\text{sec}$ and the thickness of pentacene film was about 1000 \AA , monitored by the quartz crystal oscillator. Slower deposition rate is expected to result in smoother and better ordering of the organic molecules. The deposition temperature is also a factor influencing the pentacene film formation. The temperature we use in depositing pentacene films is $70 \text{ }^\circ\text{C}$. We use shadow mask to define the active region of each device.

Step6. Patterned pentacene

As shown in Fig. 2.4, dipped in solution and the pentacene film was removed. This process clearly removed the unwanted disordered pentacene film around the channel region.

Step7. Source/Drain deposition through the shadow mask

The injection barrier of the OTFT device is determined by the materials of the source and drain electrodes. Materials with large work function are preferred to form Ohmic contact

[61]. The Au with work function $\sim 5.1\text{eV}$ does help to provide a better injection. Then, we deposited Au as the source/drain electrodes on the pentacene film. The thickness of the electrode pad is 1000\AA .

The top contact structure is shown in figure 1-7(a). In this study, all the measured data were obtained from the semiconductor parameter analyzer (HP 4156A) in the darks at room temperature. And we measure the OTFTs immediately when the samples were unloaded from the evaporation chamber.



2.2 Methods of Device parameters extraction

We measured all the device characteristics in the darks at room temperature. In this experiments, we compare devices with channel length in different structures. The channel width is 600 μm and length is 50~500 μm . We provide the drain voltage from 0 to -30V and change the gate voltage from 0 to -30V, step by -5V. The I_D - V_D curves show the turn-on operation of the device. In transfer characteristics (I_D - V_G), the gate bias ranged from 20 to -40V, and the drain voltage (-5V to -30V) are provided for the device with 1000 \AA film. From the transfer characteristics data, we can extract the mobility and threshold voltage from the square-root of drain current and transconductance.

In this section, the methods of extraction the mobility, the threshold voltage, the on/off current ratio, the subthreshold swing, the maximum interface trap density, and the surface free energy is characterized, respectively.

2-2-1 Mobility

Generally, mobility can be extracted from the transconductance maximum g_m in the linear region:

$$g_m = \left[\frac{\partial I_D}{\partial V_G} \right]_{V_D = \text{constant}} = \frac{WC_{OX}}{L} \mu V_D \quad (2.1)$$

Mobility can also be extracted from the slope of the curve of the square-root of drain current versus the gate voltage in the saturation region, i.e. $-V_D > -(V_G - V_{TH})$:

$$\sqrt{I_D} = \sqrt{\frac{W}{2L} \mu C_{ox} (V_G - V_{TH})} \quad (2.2)$$

2-2-2 Threshold voltage

Threshold voltage is related to the operation voltage and the power consumptions of an OTFT. We extract the threshold voltage from equation (2.2), the intersection point of the square-root of drain current versus gate voltage when the device is in the saturation mode operation.

2-2-3 On/Off current ratio

Devices with high on/off current ratio represent large turn-on current and small off current. It determines the gray-level switching of the displays. High on/off current ratio means there are enough turn-on current to drive the pixel and sufficiently low off current to keep in low power consumption.

2-2-4 Subthreshold swing

Subthreshold swing is also important characteristics for device application. Its is a measure of how rapidly the device switches from the off state to the on state in the region of exponential current increase. Moreover, the subthreshold swing also represents the interface quality and the defect density [62].

$$S = \left. \frac{\partial V_G}{\partial (\log I_D)} \right|_{V_D = \text{constant}}, \text{ when } V_G < V_T \text{ for p-type.} \quad (2.3)$$

If we want to have good performance TFTs, we need to lower subthreshold swing of transistors.

2-2-5 Surface free energy

The surface-free-energy of gate dielectrics is a characteristics factor, which affects the performance of the OTFTs. The surface-free-energy was calculated from the contact-angle measurement. In our experiments, the surface energy was extracted by some different calculating methods.

For the most part of the surface energy extracted methods, the Fowkes and Young approximation was used. As shown in the following equation [63]:

$$(1 + \cos \theta) \gamma_L = 2(\gamma_S^d \gamma_L^d)^{1/2} + 2(\gamma_S^p \gamma_L^p)^{1/2} \quad (2.4)$$

where θ is the contact angle between probing liquid and solid surface; γ_L , γ_L^d and γ_L^p is the total surface-free-energy, dispersion, and polar component of probing liquid, respectively. From this approximation, the total surface free energy γ_S of the solid surface is:

$$\gamma_S = \gamma_S^d + \gamma_S^p$$

It is characterized by the sum of dispersion γ_S^d and polar γ_S^p components.

Chapter 3

Experiments Results and Discussion

3.1 Self-Assembly Monolayer (SAM)

In this study, we introduce Self-Assembled Monolayer-ODMS as the surface treatment material (see Figure. 1.6). First, we selected several solvents such as alcohol, toluene, acetone, and isopropyl alcohol to mix with ODMS into several concentrations to make comparisons. As shown in Figure. 3.1,3.2 from the contact angle and surface energy measured from the solvent, it can be known that alcohol and toluene reveal better traits. From the experiment results of the solvents comparison, it can be known that alcohol solvent has better results than the toluene solvent. Therefore, we selected alcohol as the solvent in mixing with ODMS. After selecting the solvent, we select the optimal concentration. As shown in Figure 3.3 and Table II, some different of concentration was used to measure the contact angle. As the experiment result presents the concentration of 10 mM would achieve the largest contact angle.

3.2 Surface energy control

An attempt was made to control the surface polarity by exposure to UV light. First, the silicon oxide was dipped in the dissolved liquid ODMS to let the surface of the silicon oxide be a hydrophobic one. Then, expose the dielectric surface treated with ODMS under 1 minute, 3 minutes, 15 minutes, 30 minutes, and no exposure to UV light.; these are the different conditions. As shown in Figure 3.4, the contact angle and surface free energy was controlled by the exposing time of the UV-light. To extract the surface free energy of the dielectric surface, the Fowkes and Young approximation [64, 65].

OTFTs fabricated under several conditions were classified as follows. To serve as a control, OTFTs fabricated by conventional process without ODMS treatment or UV light exposure was labeled as conventional devices. The devices with different conditions are schematically presented in Figure. 2.3 and Table III.

As shown in Fig. 3.4, the solid line represents the contact angle of the de-ionized water on dielectric surface. Before UV light exposure, it was about 30.4 degree and 90 degree on bare SiO₂ surface and on ODMS-treated SiO₂ surface, respectively. Apparently, the ODMS transformed the SiO₂ surface from hydrophilic to hydrophobic. After being illuminated by the UV-light, the contact angle decreased rapidly with time. After 600-second exposure, the contact angle dropped to be around 30 degree. After 25-minutes exposure, the contact angle approached the limitation of the measurement instrument and is around 5 ± 5 degree. The

UV light efficiently destroyed the organic film (means ODMS in this study) and altered the surface polarity [66]. The UV light excites chemical bonds, such as. C-C, C-H, and C-Si, and forms radicals [66]. Such radicals are actively oxygen species such as ozone or atomic oxygen, generated by the excitation of atmospheric oxygen molecules by UV: [66]



Accordingly, ODMS molecules might be converted to volatile species such as CO₂ and H₂O that could be removed immediately[66].

The contact angle variation represented the change of surface energy. The surface energy could be calculated by the Fowkes and Young approximation, as in the following equation;

[66, 67]

$$(1 + \cos \theta)\gamma_L = 2(\gamma_S^d \gamma_L^d)^{1/2} + 2(\gamma_S^p \gamma_L^p)^{1/2} \quad (3.2)$$

where θ was the measured contact angle; γ_L was the surface free energy of the testing liquid and was the sum of its dispersion part γ_L^d and its polar part γ_L^p ; γ_S^d and γ_S^p were the dispersion and polar component of the surface free energy of the solid surface. To obtain the values of γ_S^d and γ_S^p , the contact angle of three standard liquids (DI water, diiodo-Methane and Ethylen glycol) should be measured. The measurement result was shown in the inset of Fig. 3.4(a). By knowing the γ_L^d and γ_L^p of these standard liquids, the γ_S^d and γ_S^p of the dielectric surface could be calculated. Also, the total surface free energy of the solid γ_S can be estimated by

$$\gamma_s \cong \gamma_s^p + \gamma_s^d \quad (3.3)$$

Figure 3.4(b) depicted the calculated results of γ_s^d , γ_s^p and γ_s . It was found that UV light illumination changed mostly the polar component of the dielectric surface.

Finally, electric characteristics analysis can prove a significant difference after exposure to UV light. As in Figure 3.5 (a), increase of UV light exposure time causes a significant degeneration of performance. After ODMS treatment, surfaces exposed to 30 minutes of UV light exposure have electric characteristics similar to those of conventional OTFTs. This implied that, after 30-mins UV exposure, the ODMS layer was destroyed.



3.3 OTFTs with patterned pentacene

A patterning method for pentacene film is proposed. This method was realized by self-assembled layer (SAM) and ultra-violet (UV) light post-exposure. The surface characteristic on the gate dielectric is controlled. The difference of the interfacial binding energy between the pentacene film and the dielectric enables the pentacene film to be removed selectively. The remaining pentacene film was fabricated as a top-contact OTFT to confirm the practicability of this experiment.

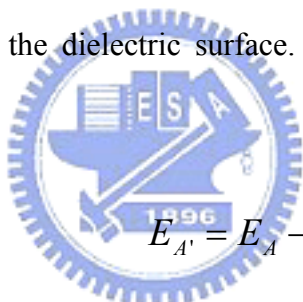
Figure 3.6 (a) showed the AFM images of the pentacene deposited on the non-UV-exposed and on 30-mins UV-exposed regions. The latter had larger grain size than the former; this agrees with the results in Ref 70 that pentacene formed larger grain on the surface with higher surface energy. The difference of the surface energy also led to different results after the water dipping. As shown by the AFM image in Figure 3.6 (b), after dipping, pentacene film on the non-UV-exposed area was almost unchanged while it on the 30-mins UV-exposed area was removed. The step of this two area was about 100 nm, similar to the thickness of the pentacene film. This implied that the pentacene film was almost completely removed.

An attempt was made to characterize the adhesive properties between the pentacene film and the substrate surface to study the patterning mechanism. The adhesion energy between different materials as the following equations were reported by D.H. Kaelble[68]

$$E_A = 2(\sqrt{\gamma_{pe}^p \gamma_s^p} + \sqrt{\gamma_{pe}^d \gamma_s^d}) \quad (3.4)$$

where E_A was the adhesion energy between pentacene and substrate before water dipping; γ_{pe}^p and γ_{pe}^d were the polar component and the dispersion component of the surface energy for pentacene; γ_s^p and γ_s^d were the polar component and the disperse component of the surface energy for the substrate. As shown in Figure 3.7, the adhesion energy before water dipping was slightly increased after UV-light exposure. This was an interesting result since increased adhesion energy could not explain the water-removable property.

Therefore, we calculated and compared the intrusion energy E_I caused by the interaction between water, pentacene and the dielectric surface. This intrusion energy would cause a change of adhesion energy by:



$$E_{A'} = E_A - E_I \quad (3.5)$$

where the $E_{A'}$ was the adhesion energy after water dipping.

The intrusion energy could be calculated by the method of D.H. Kaelble. The calculated intrusion energy E_I and the adhesion energy after water dipping $E_{A'}$ were also depicted in Fig. 3.7. The E_I increased drastically after UV light exposure, as a result, the $E_{A'}$ decreased to be less than zero after UV exposure. Specifically, the $E_{A'}$ of non-UV-exposed region was 58 mJ/m² and that of 30-mins UV-exposed region was -38 mJ/m². This explained the experimental results in Figure 3.6 (b). Pentacene film on non-UV-exposed area was almost unaffected due to the large $E_{A'}$; pentacene film on 30-mins UV exposed area was removed by

water dipping due to the negative $E_{A'}$. Also, the large difference of the $E_{A'}$ between non-UV-exposed area and UV-exposed area explained the capability to successfully pattern the pentacene film.

Finally, the electric characteristics were demonstrated to confirm that the patterning method was feasible for the OTFTs. Figure 3.8 (a) compared the transfer characteristics of OTFTs under different conditions. The performance of ODMS-treated OTFTs was greatly improved when compared with conventional devices without ODMS treatment. Next, when comparing pentacene patterning - OTFTs and the ODMS-treated OTFTs, the former showed a bit right-hand side shift characteristics and a higher minimum off state current. This influence of some residual water molecules might be the plausible reason. However, After pentacene patterning, performance of ODMS treated OTFTs nearly all still maintain good electric characteristics. The mobility as $0.264 \text{ cm}^2/\text{V}\cdot\text{s}$ and I_{on}/I_{off} ratio higher than 6 orders were still obtained.

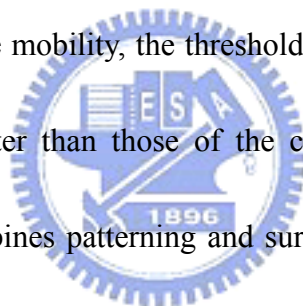
Typical parameters such as mobility, threshold voltage, on/off current ratio and sub-threshold swing of these devices were listed in Table IV. The output characteristics of pentacene patterning - OTFTs was also depicted in Figure 3.8 (b). No hysteresis was observed when the drain voltage was scanned from 0 (V) to -30 (V) and then from -30 (V) to 0 (V).

Chapter 4

Conclusion

A novel technology for patterning pentacene-OTFTs was proposed. ODMS-SAM and the following UV-light exposure were used to modulate the surface energy of the dielectric. The SiO₂ gate dielectric with ODMS treatment exhibited low surface energy as 41mJ/m². The surface energy increased drastically when the ODMS-treated dielectric surface was irradiated by UV light. After 30-mins UV exposure, the surface energy increased to be 155mJ/cm².

The pentacene film was therefore controlled and patterned by the difference of the dielectric surface energy. The mobility, the threshold voltage, the on/off current ratio and the sub-threshold swing were better than those of the control sample, even following solution process. Technology that combines patterning and surface treatment may be applied to future OTFTs arrays.



References

- [1]. M. Pope and C.E. Swenberg, *Electronic Processes in Organic Crystals and Polymers* (Oxford University Press, New York, 1999).
- [2] A. Tsumura, K. Koezuka, and T. Ando, “Macromolecular electronic devices: Field-effect transistor with a polythiophene thin film”, *Appl. Phys. Lett.* vol.49, pp. 1210, (1986).
- [3]. D.F. Barbe and C.R. Westgate: Surface state parameters of metal-free phthalocyanine single crystals. *J. Phys. Chem. Solids* **31**, 2679 (1970).
- [4]. M.L. Petrova and L.D. Rozenshtein: Field effect in the organic semiconductor chloranil. *Fiz. Tverd. Tela (Soviet Phys. Solid State)* **12**, 961 (1970).
- [5]. M.L. Petrova and L.D. Rozenshtein: Field effect in the organic semiconductor chloranil. *Fiz. Tverd. Tela (Soviet Phys. Solid State)* **12**, 961 (1970).
- [6] A. Tsumura, K. Koezuka, and T. Ando, “Macromolecular electronic devices: Field-effect transistor with a polythiophene thin film”, *Appl. Phys. Lett.* vol.49, pp. 1210, (1986).
- [7] J. H. Burroughes, C. A. Jones, and R. H. Friend, “Polymer diodes and transistors: new semiconductor device physics”, *Nature*, vol. 335, pp.137, (1988).
- [8] A. Tsumura, K. Koezuka, and T. Ando, “Macromolecular electronic devices: Field-effect transistor with a polythiophene thin film”, *Appl. Phys. Lett.* Vol.49, pp. 1210, (1986)
- [9]. F. Ebisawa, T. Kurokawa, and S. Nara: Electrical properties of polyacetylene-polysiloxane interface. *J. Appl. Phys.* **54**, 3255 (1983).
- [10]. A. Tsumura, K. Koezuka, and T. Ando: Macromolecular electronic device: Field-effect transistor with a polythiophene thin film. *Appl. Phys. Lett.* **49**, 1210 (1986).
- [11]. H. Shirakawa, E.J. Louis, A.G. MacDiarmid, C.K. Chiang, and A. Heeger: Synthesis of electrically conducting organic polymers: Halogen derivatives of polyacetylene, (CH)_x. *J. Chem. Soc. Chem. Commun.* **00**, 578 (1977).
- [12] R. Smith, D. Allee, C. Moyer, and D. Loy, “Flexible Transistor Arrays”, *SID* 21, 18,

(2005)

- [13]. G. Horowitz, D. Fichou, X.Z. Peng, Z.G. Xu, and F. Garnier: A field-effect transistor based on conjugated alpha-sexithienyl. *Solid State Commun.* **72**, 381 (1989).
- [14]. C.W. Tang and S.A. van Slyke: Organic electroluminescent diodes. *Appl. Phys. Lett.* **51**, 913 (1987).
- [15]. J.H. Burroughes, D.D.C. Bradley, A.R. Brown, R.N. Marks, K. Mackay, R.H. Friend, P.L. Burns, and A.B. Holmes: Lightemitting diodes based on conjugated polymers. *Nature* **341**, 539 (1990).
- [16]. H.E. Katz: Organic molecular solids as thin film transistor semiconductors. *J. Mater. Chem.* **7**, 369 (1997). 16. A.R. Brown, C.P. Jarrett, D.M. de Leeuw, and M. Matters: Fieldeffect transistors made from solution-processed organic semiconductors. *Synth. Metal* **88**, 37 (1997).
- [17]. F. Garnier: Thin-film transistors based on organic conjugated semiconductors. *Chem. Phys.* **227**, 253 (1998).
- [18]. G. Horowitz: Organic field-effect transistors. *Adv. Mater.* **10**, 365 (1998).
- [19]. C.D. Dimitrakopoulos and P.R.L. Malenfant: Organic thin film transistors for large area electronics. *Adv. Mater.* **14**, 99 (2002).
- [20] C. D. Dimitrakopoulos, D. J. Mascaro, "Organic thin-film transistors: a review of recent advances", *IBM J. Res. Dev* 45, 11-27, (2001)
- [21] C. Reese, M. Roberts, Mang-mang Ling, and Z. Bao, "Organic thin film transistors", *Materialstoday*, Vol. 7, pp. 20-27, (2004)
- [22] C.W. Chu, S.H. Li, C.W. Chen, V. Shrotriya, Y. Yang, "High-performance organic thin-film transistors with metal oxide/metal bilayer electrode" , *Applied Physics Letters*, Vol. 87, pp.193508, (2005)
- [23] K. Puntambekar, J. Dong, G. Haugstad, C.D. Frisbie, "Structural and electrostatic complexity at a pentacene/insulator interface" , *Adv. Funct. Mater*, Vol.16, pp.679 (2006)

- [24] M. Kawasaki, S. Imazeki, M. Ando, Y. Sekiguchi, S. Hirota, "High-resolution full-color LCD driven by OTFTs using novel passivation film", IEEE Transactions on Electron Devices, Vol. 53, pp. 435- 441, (2006)
- [25] K. Tsukagoshi, J. Tanabe, I. Yagi, K. Shigeto, "Organic light-emitting diode driven by organic thin film transistor on plastic substrates", Journal of Applied Physics, Vol. 99, pp.064506
- [26] Y. Y. Lin, D. J. Gundlach, S. F. Nelson, and T. N. Jackson, "Pentacene organic thin-film transistors-molecular ordering and mobility", IEEE Electron Device Lett. vol. 18, pp. 87, (1997).
- [27] C. D. Dimitrakopoulos and P. R. L. Malenfant, "Organic thin film transistors for large area electronics", Adv. Mater. (Weinheim, Ger.) 14, No. 2, pp.99, (2002).
- [28] L. Torsi, A. Dodabalapur, L. J. Rothberg, A. W. P. Fung, H.E. Katz, "Performance Limits of Organic Transistors", Science, 1996, P 1462.
- [29] H. E. Katz, C. Kloc, V. Sundar, J. Zaumseil, A. L. Briseno, Z. Bao, "Field-Effect Transistors made from Macroscopic Single Crystals of Teracene and Related Semiconductors on Polymer Dielectrics", Journal of Material Research, Vol. 19, No. 7, Jul 2004, P 1995 - 1998.
- [30] C. D. Dimitrakopoulos, D. J. Mascaro, "Organic Thin-Film Transistors: A Review of Recent Advances", IBM Journal of Research and Development, Vol. 45, No. 1, Jan 2001, P 11 - 27.
- [31] Z. Bao, A. Dodabalapur, A. J. Lovinger, "Soluble and processable regioregular poly(3-hexylthiophene) for thin film field-effect transistor applications with high mobility" Appl. Phys. Lett. Vol. 69, pp.4108, (1996)
- [32] Y.Y. Lin, D. J. Gundlach, S. Nelson, T. N. Jackson, "Stacked pentacene layer organic thin-film transistors with improved characteristics", IEEE Electron Device Lett, Vol. 18, pp.606, (1997).

- [33] Yanming Sun, Yunqi Liu, and Daoben Zhu, “Advances in organic field-effect transistors”, *J. Mater. Chem.*, vol. 15, pp. 53, (2005).
- [34] G. M. Wang, J. Swensen, D. Moses, and A. J. Heeger, “Increased mobility from regioregular poly (3-hexylthiophene) field-effect transistors”, *J. Appl. Phys*, Vol 93, pp 6137, (2003)
- [35] L. Sebastian, G. Weiser, and H. Bassler, “Charge transfer transitions in solid tetracene and pentacene studied by electroabsorption”, *Chemical Physics*, Vol 61, pp 125-135, (1981)
- [36] E. A. Silinsh, and V. Capek, “Organic Molecular Crystals: Their Electronic States “, New York, (1980)
- [37] Y. S. Yang, S. H. Kim, J. Lee, H.Y. Chu, L. Do, “Deep-level defect characteristics in pentacene organic thin films”, *Applied Physics Letters*, Vol. 80, pp. 1595-1597, (2002)
- [38] H. Yanagisawa, T. Tamaki, M. Nakamura, K. Kudo, “Structural and electrical characterization of pentacene films on SiO₂ grown by molecular beam” *Thin Solid Films*, Vol. 464-465, pp.398, (2004)
- [39] D. Knipp, R. A. Street, A. Vo^o lkel, J. Ho. “Pentacene thin film transistors on inorganic dielectrics: Morphology, structural properties, and electronic transport” *Journal of Applied Physics*, Vol. 93, pp.247, (2003)
- [40] R. A. Street, D. Knipp, and A. R. Vo^l kel, “Hole transport in polycrystalline pentacene transistors”, *Appl. Phys. Lett.*, vol. 80, pp. 1658, (2002).
- [41] G. Horowitz, “Organic field-effect transistors”, *Adv. Mater.*, vol. 10, pp. 365, (1998).
- [42] Y.-Y. Lin, D. J. Gundlach, S. F. Nelson, and T. N. Jackson, “Stacked pentacene layer organic thin-film transistors with improved characteristics”, *IEEE Electron Device Lett*, vol. 18, pp 606, (2000).
- [43] S. F. Nelson, Y.-Y. Lin, D. J. Gundlach, and T. N. Jackson, “Temperature-independent transport in high-mobility pentacene transistors”, *Appl. Phys. Lett.*, vol. 72, pp. 1854, (1998).

- [44] O. Ostroverkhova, D. G. Cooke, S. Shcherbyna, R. F. Egerton, F. A. Hegmann, R. R. Tykwinski, and J. E. Anthony, "Bandlike transport in pentacene and functionalized pentacene thin films revealed by subpicosecond transient photoconductivity measurements", *Phys. Rev. B*, vol. 71, pp. 035204, (2005).
- [45] G. Nunes Jr., S. G. Zane, and J. S. Meth, "Styrenic polymers as gate dielectrics for pentacene field-effect transistors", *J. Appl. Phys.*, vol. 98, pp. 104503, (2005).
- [46] M. McDowell, I. G. Hill, J. E. McDermott, S. L. Bernasek, and J. Schwartz, "Improved organic thin-film transistor performance using novel self-assembled monolayers", *Appl. Phys. Lett.*, vol. 88, pp. 073505, (2006).
- [47]. R.H. Tredgold, *Order in Thin Organic Films*, Cambridge University Press, 1994.
- [48] A. Ulman, *An Introduction to Ultrathin Organic Films: From Langmuir-Blodgett to Self-Assembly*, Academic press, New York, 1991.
- [49]. R.F. Gould (Ed.), *Contact Angle, Wettability and Adhesion*, Proceeding of the 144th Meeting of the American Chemical Society, Vol. 43, Washington, DC, 1964.
- [50]. R.J. Good, *Contact angle wetting and adhesion: a critical review*, in: K.L. Mimal (Ed.), *Contact angle, Wettability and Adhesion*, USP, The Netherlands, 1993, pp. 3–36.
- [51] M. McDowell, I. G. Hill, J. E. McDermott, S. L. Bernasek, and J. Schwartz, *Appl. Phys. Lett.*, Vol. 88, pp.073505 (2006)
- [52] A. Inoue, T. Ishida, and N. Choi, *Appl. Phys. Lett.* 73,14 (1998)
- [53] D. R. Hines, S. Mezhenny, M. Breban, and E. D. Williams, *Appl. Phys. Lett.* 86, 163101 (2005)
- [54] Sung Hwan Kim, Hye Young Choi, Seung Hoon Han, Ji Ho Hur and Jin Jang, *SID DIGEST Section 45.2* p.1297 (2004).
- [55] Masahiko Ando, Masahiro Kawasaki, Shuji Imazeki, Hiroshi Sasaki, and Toshihide Kamata, *Appl. Phys. Lett.*, Vol. 85, pp.1849 (2004)
- [56] Wakana Kubo and Tetsu Tatsuma, *Apply. Surf. Sci.* 243 125 (2005)

- [57] A. R. Brown, C. P. Jarrett, D. M. de Leeuw, and M. Matters, "Field-effect transistors made from solution-processed organic semiconductors", *Synth. Met.*, vol. 88, pp. 37, (1997).
- [58] T. Torsi, "Novel applications of organic based thin film transistors", *Solid-State Electronics*, Vol 45, pp 1479-1485, (2001)
- [59] Sung Hwan Kim, Hye Young Choi, Seung Hoon Han, Ji Ho Hur and Jin Jang, *SID DIGEST Section 45.2* p.1297 (2004)
- [60] C. D. Dimitrakopoulos, A. R. Brown, and A. Pomp, "Molecular beam deposited thin films of pentacene for organic field effect transistor applications", *J. Appl. Phys.*, vol. 80, pp. 2501, (1996).
- [61] Chih-Wei Chu, Sheng-Han Li, Chieh-Wei Chen, Vishal Shrotriya, and Yang Yang, "High-performance organic thin-film transistors with metal oxide/metal bilayer electrode", *Appl. Phys. Lett.*, vol. 87, pp. 193508, (2005).
- [62] K N Narayanan Unni, Sylvie Dabos-Seignon, and Jean-Michel Nunzi, "Improved performance of pentacene field-effect transistors using a polyimide gate dielectric layer", *J. Phys. D: Appl. Phys.*, vol. 38, pp. 1148, (2005).
- [63] Kui-Xiang Ma, Chee-Hin Ho, Furong Zhu, and Tai-Shung Chung, "Investigation of surface energy for organic light emitting polymers and indium tin oxide", *Thin Solid Films*, vol. 371, pp. 140, (2000)
- [64] *Surface, Interfaces, and Colloids* ; Drew Myers ; New York, 1999.
- [65] Fowkes, F. M. *J Phys Chem* 67, 2538. (1963)
- [66] H Sugimura, N Saito, N Maeda, I Ikeda, Y Ishida, K Hayashi, L Hong, and O Takai, *Nanotechnology* 15 s69-s75(2004)
- [67] Sang Yoon Yang, Kwonwoo Shin, and Chan Eon Park, *Adv. Mater.* 15,1806 (2005)
- [68] D. H. Kaelble, *J. of Applied Polymer Science* 18, 1869 (1974).

Table I Comparisons of TFTs using different materials.

	Amorphous Si	Poly-Si	Organic
Status	Mature	Development	Research
TFT type	N-TFT	N-TFT or P-TFT	P-TFT or N-TFT
Mobility (cm^2/Vs)	0.1-1.0	50-200	0.005-3
Uniformity	Good	Poor	Unknown
Stability	Poor	Good	Unknown
Cost	Low	High	Very low
Ion/Ioff	$>10^6$	$>10^6$	10^3-10^8
Size and voltage to drive $10\mu\text{A}$ (Gate dielectric is 300nm and channel length is $5\mu\text{m}$) (W=channel width)	W= $92\mu\text{m}$ ($V_{\text{GS}}-V_{\text{TH}}$)= 7V	W= $10\mu\text{m}$ ($V_{\text{GS}}-V_{\text{TH}}$)= 1.5V	W= $181\mu\text{m}$ ($V_{\text{GS}}-V_{\text{TH}}$)= 25V

Table II Contact angle, Surface energies and Surface roughnesses of SiO₂ treated by different ODMS concentrations.

Concentration (mM) (Alcohol mix with ODMS)	Contact angle (degree)- Water	Surface energy (mJ/ m ²)	Surface roughness (nm)
0.5	63.2	67.9	0.244
1	70.8	61.6	0.259
5	79.1	46.7	0.288
<u>10</u>	<u>82.5</u>	<u>43.6</u>	<u>0.282</u>
100	82.3	45.3	0.342

Table III Comparison of the transfer characteristics of OTFTs under different UV-exposed time.

	ODMS - treated OTFTs					Conventional device
	UV - 0 mins	UV - 1 mins	UV - 3 mins	UV - 15 mins	UV - 30 mins	
μ_{FE} (cm ² /Vs)	0.3496	0.1695	0.1179	0.0932	0.0794	0.10039
V_{TH} (V)	-20.92	-17.52	-16.53	-16.58	-16.27	-13.25
I_{on}/I_{off}	>10 ⁶	>10 ⁵	~10 ⁵	<10 ⁵	<10 ⁵	~10 ⁵
$S.S.$ (V/dec.)	0.682	2.03	2.29	2.94	3.07	2.32

Table IV Comparison of the transfer characteristics of OTFTs under different conditions.

	ODMS - treated OTFTs		Conventional device
	ODMS - treated OTFTs	Pentacene Patterned - OTFTs	
μ_{FE} (cm ² /Vs)	0.391	0.264	0.167
V_{TH} (V)	-7.34	-7.62	-6.84
I_{on}/I_{off}	~10 ⁸	>10 ⁶	>10 ⁵
$S.S.$ (V/dec.)	0.7.29	0.91	2.51

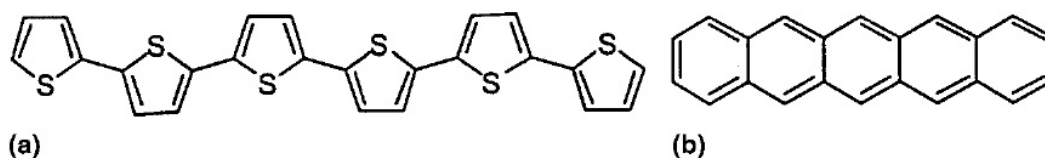


Fig. 1.1 Molecular structure of (a) sexithiophene and (b) pentacene.

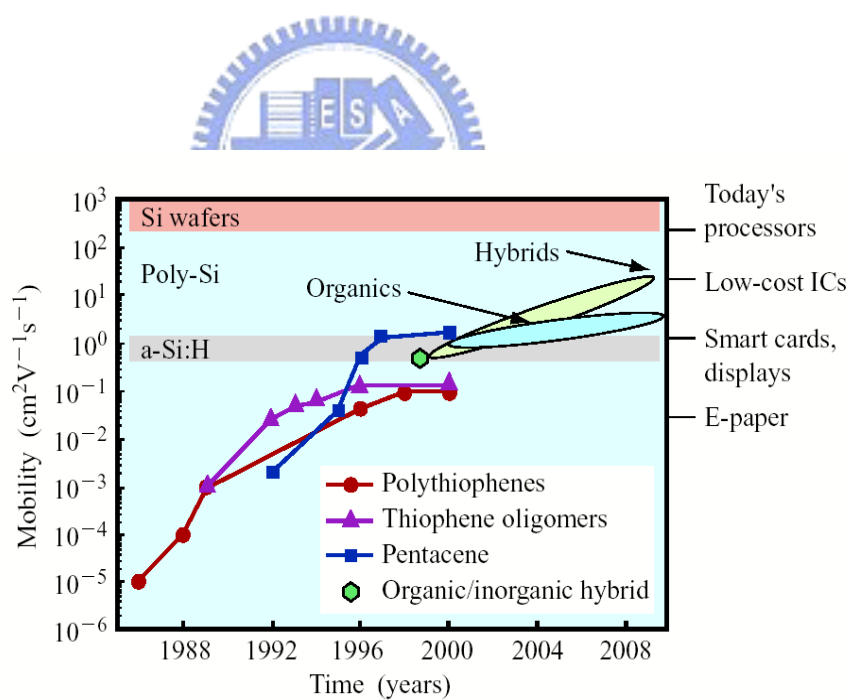


Fig. 1.2 Mobility of the organic semiconductors has been improved by five orders of magnitude over the past 15 years.

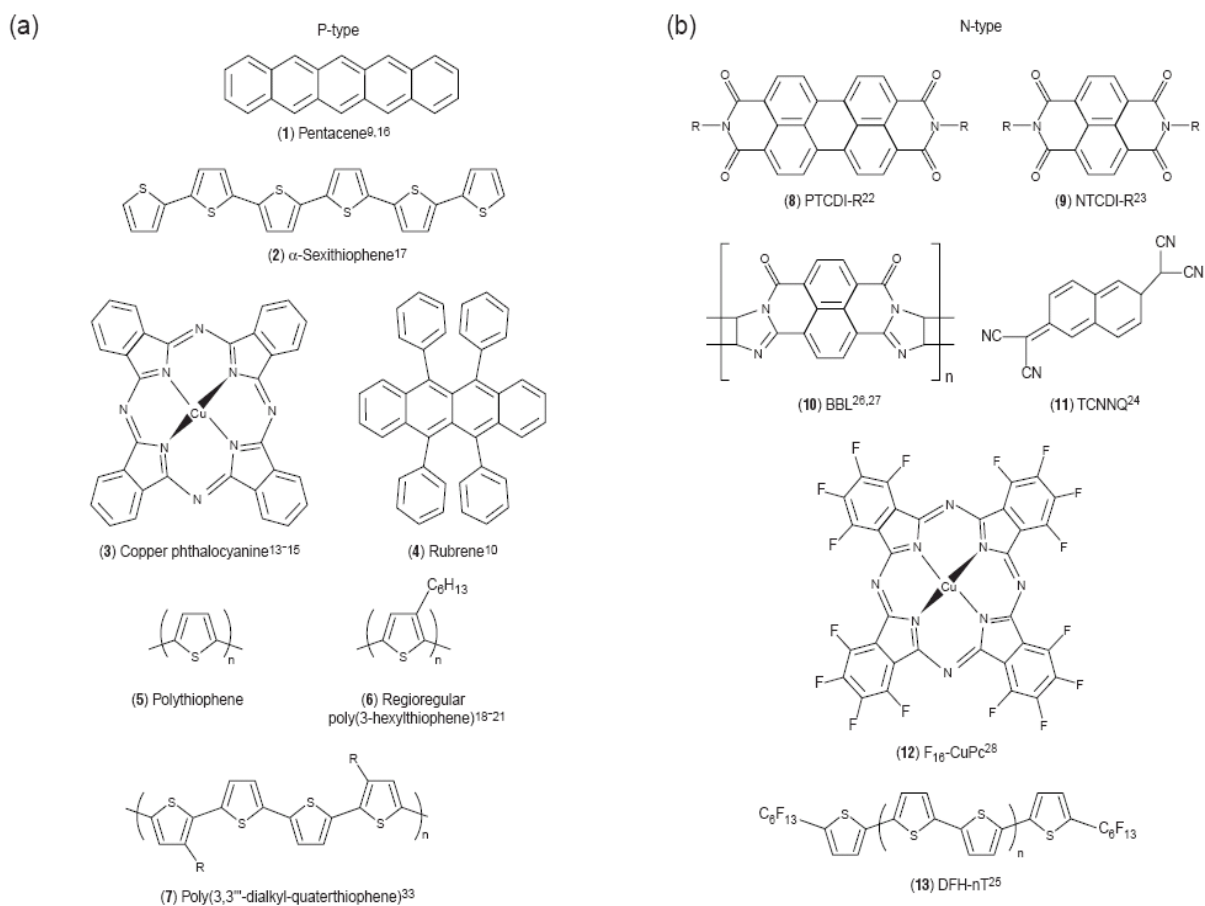


Fig. 1.3 Prominent (a) p-type and (b) n-type organic semiconductor materials

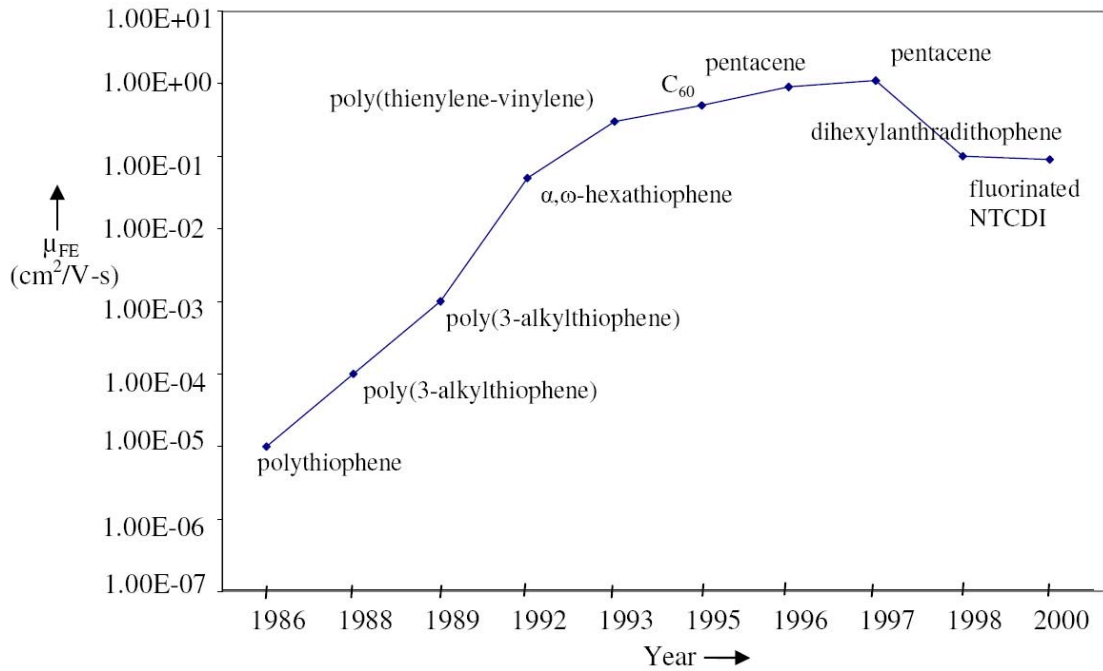


Fig. 1.4 Semilogarithmic plot of mobility vs. year.

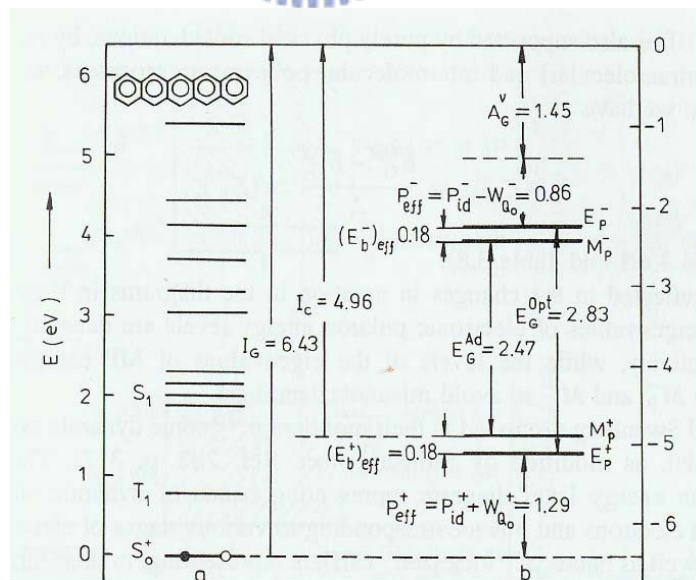


Fig. 1.5 Energy band diagram of pentacene

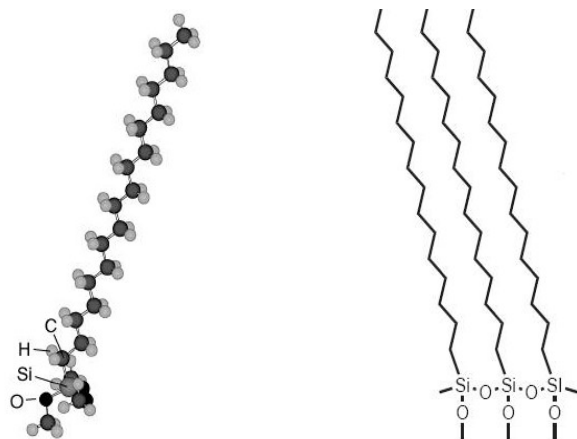
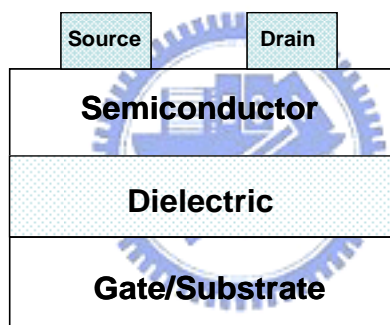


Fig. 1.6 Chemical structure of ODMS – SAMs

(a)



(b)

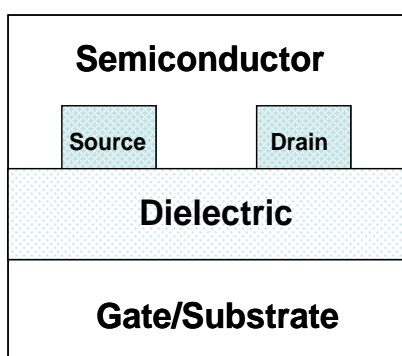
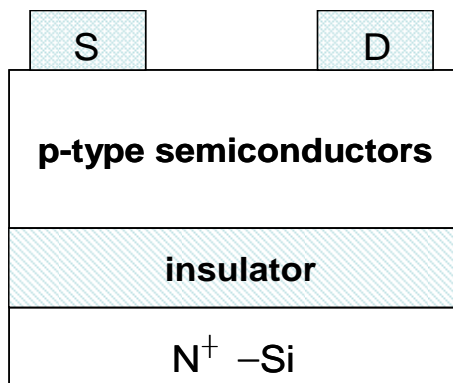
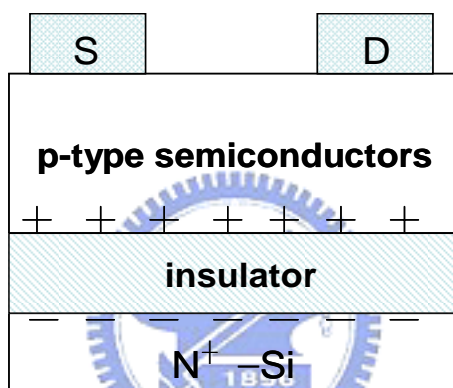


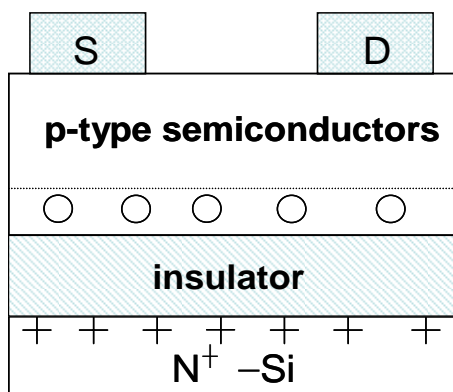
Fig. 1.7 OTFT device configurations. (a) Schematic cross section view of top contact device. (b) Schematic cross section view of bottom contact device.



(a) $V_G = V_D = 0$



(b) $V_G < V_D < 0$



(c) $V_G > 0, V_D = 0$

Fig. 1.8 Schematic of operation of OTFT, showing a p-type semiconductor: + indicates a positive charge in semiconductor; - indicate a negatively charge. (a) no-bias (b) accumulation mode (c) depletion mode.

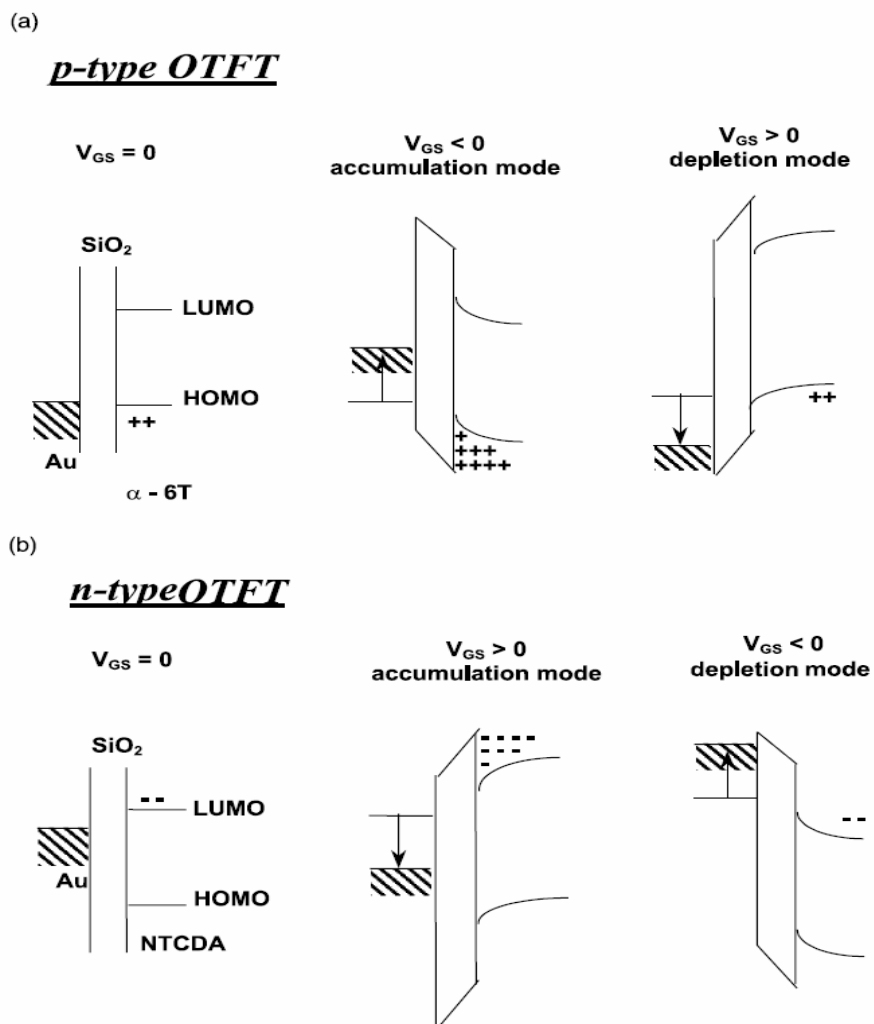


Fig. 1.9 Energy band diagrams for (a) a p-channel (pentacene) and for (b) a n-channel (NTCDA) OTFTs under different gate bias conditions.

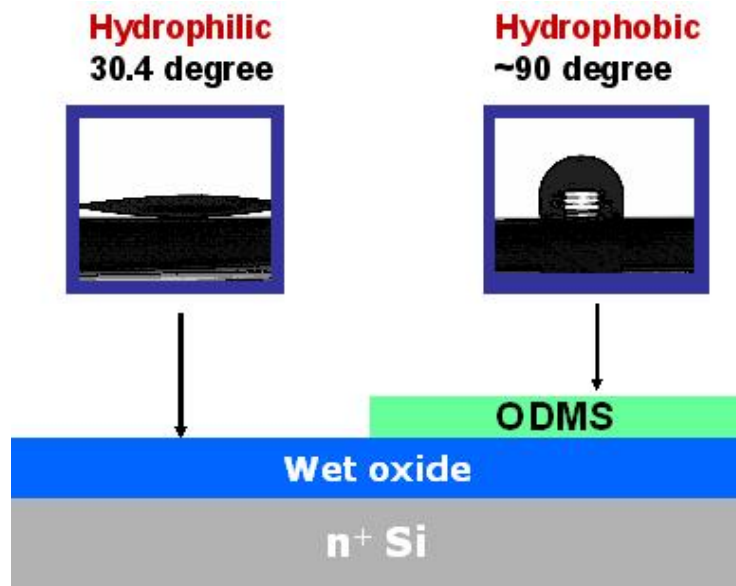


Fig. 2.1 The ODMS layer changed the gate dielectric surface from hydrophilic to hydrophobic.

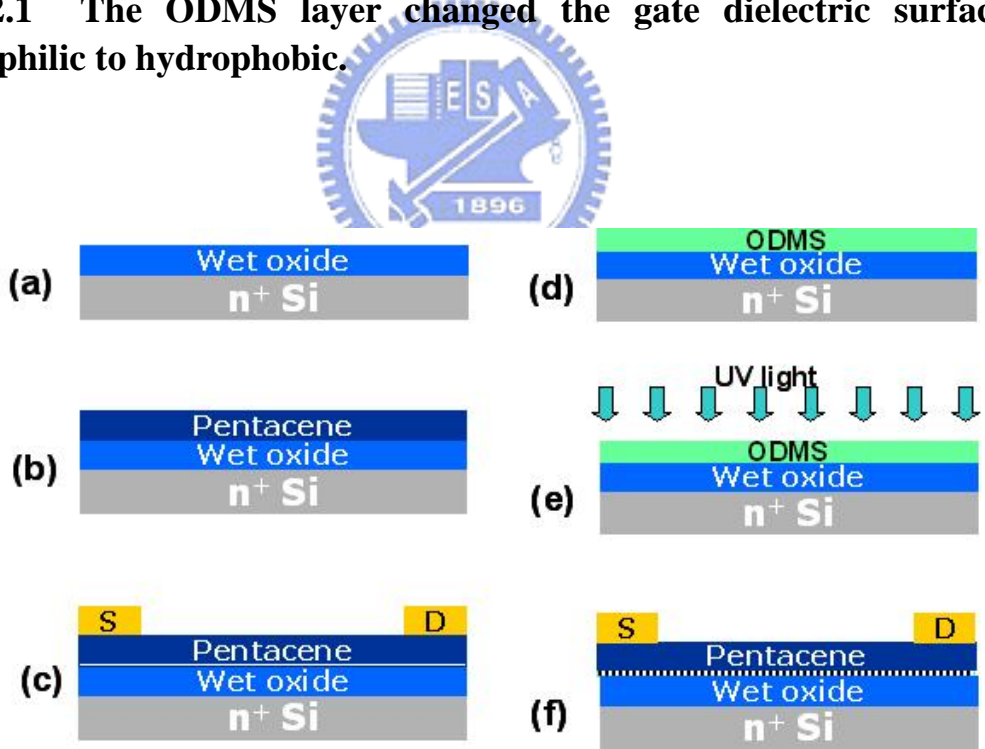


Fig. 2.2 Process flow of ODMS treatment and the ultra-violet (UV) light exposure.

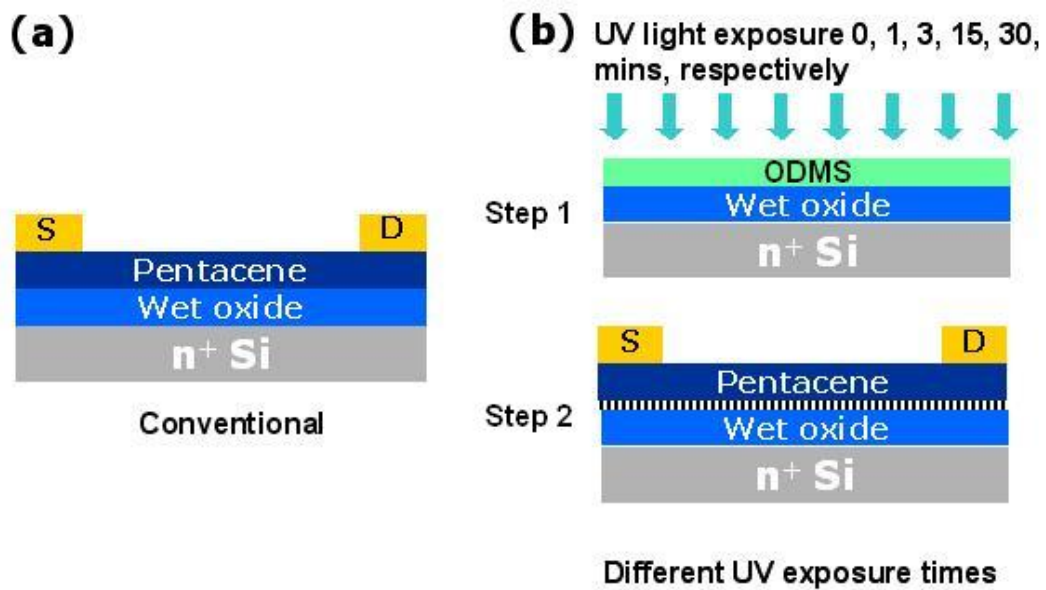


Fig. 2.3 (a) conventional OTFTs and (b) OTFTs with ODMS treatment and with different UV exposure times.

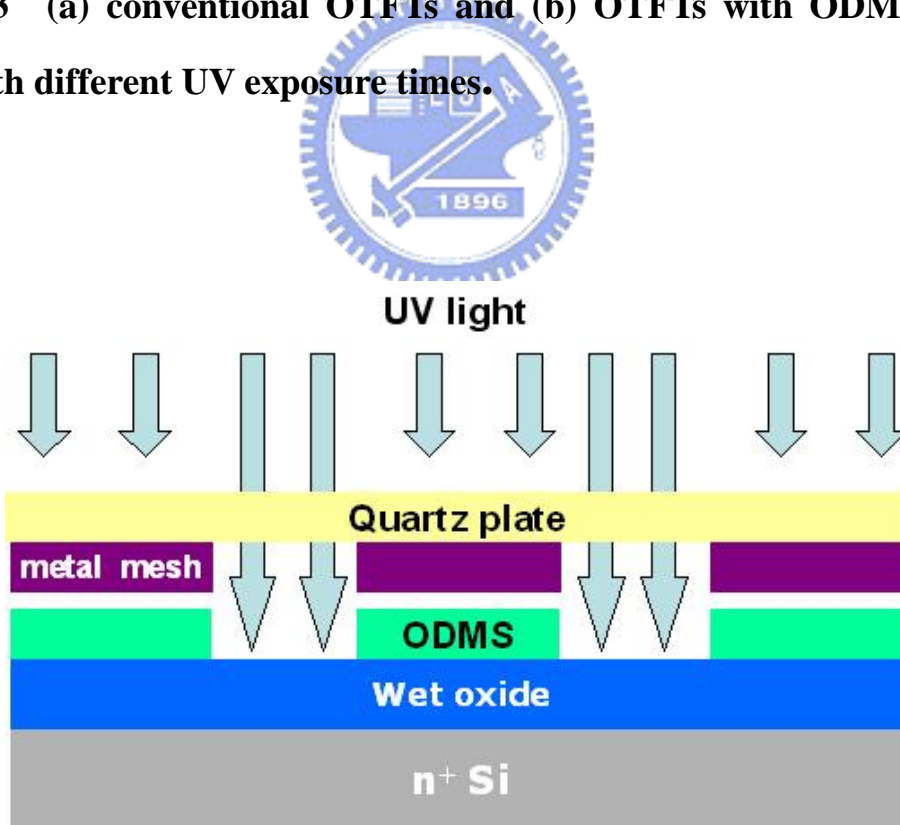


Fig. 2.4 The gate dielectric surface was partial exposed to UV light through quartz-glass mask.

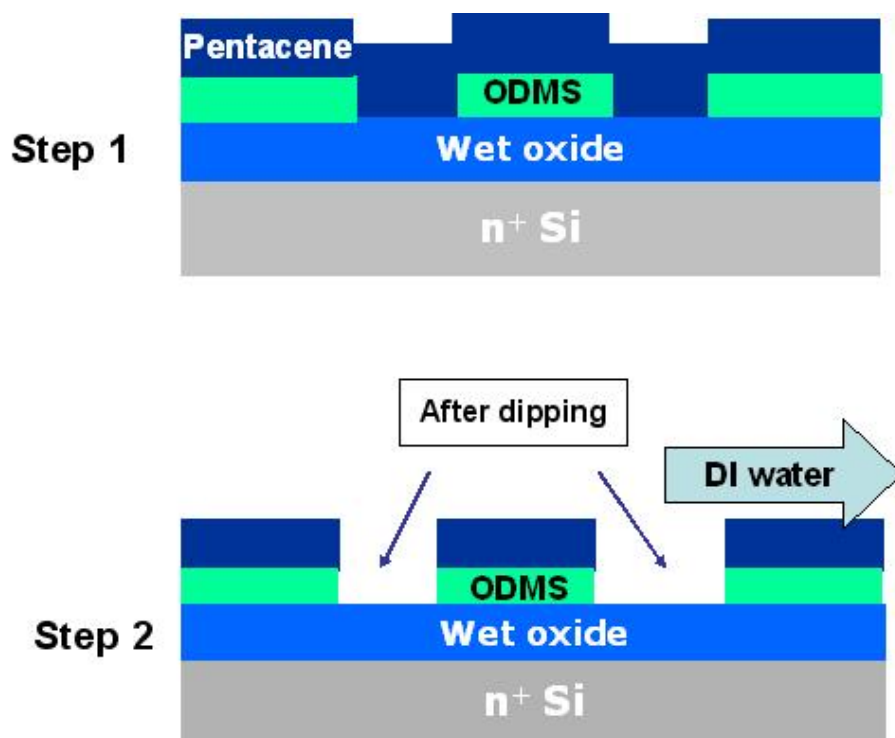


Fig. 2.5 The lift-off process for pentacene patterning.

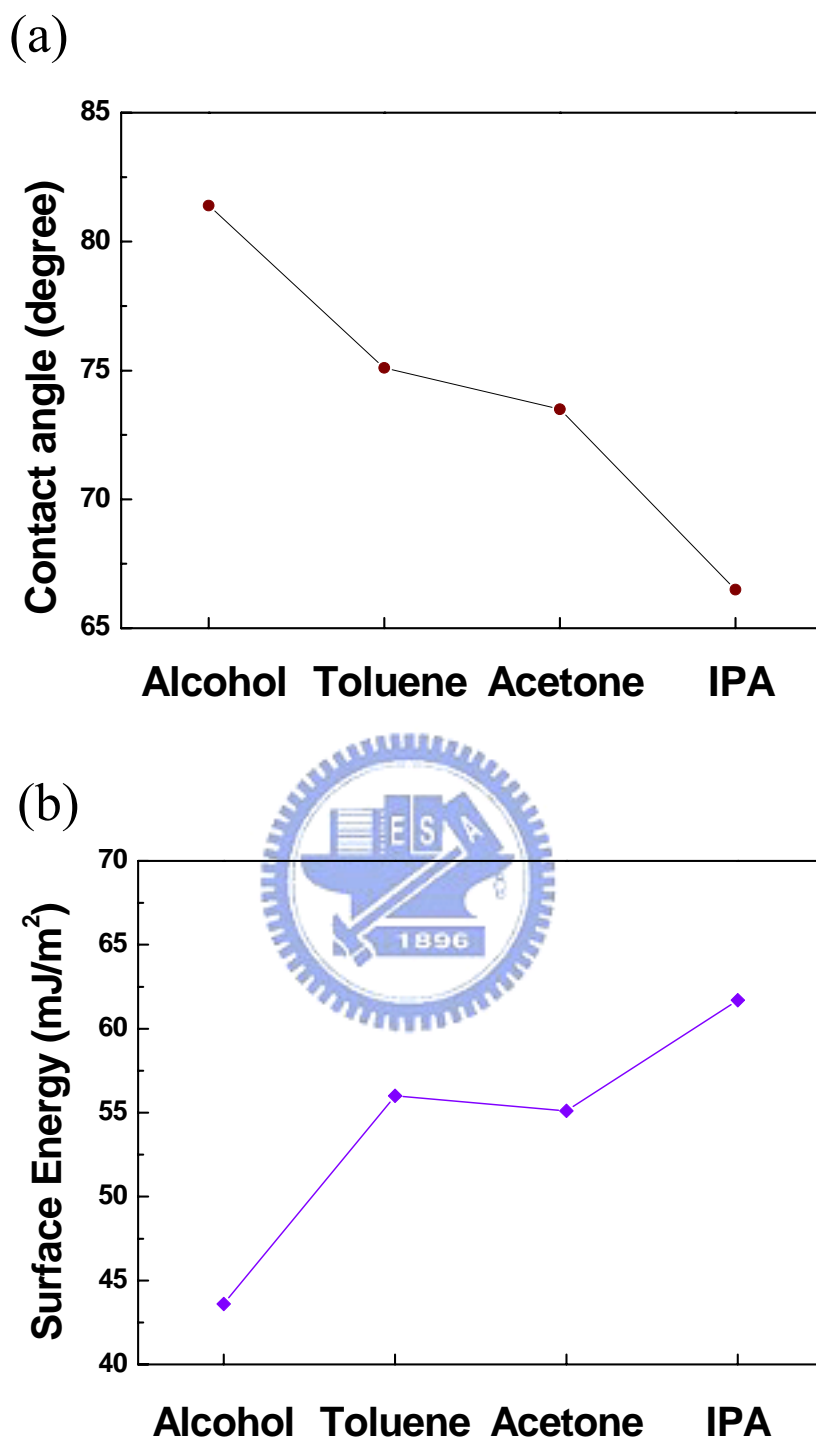


Fig. 3.1 Comparison of dielectric (a) contact angle and (b) surface energy when treated by ODMS in different solvents.

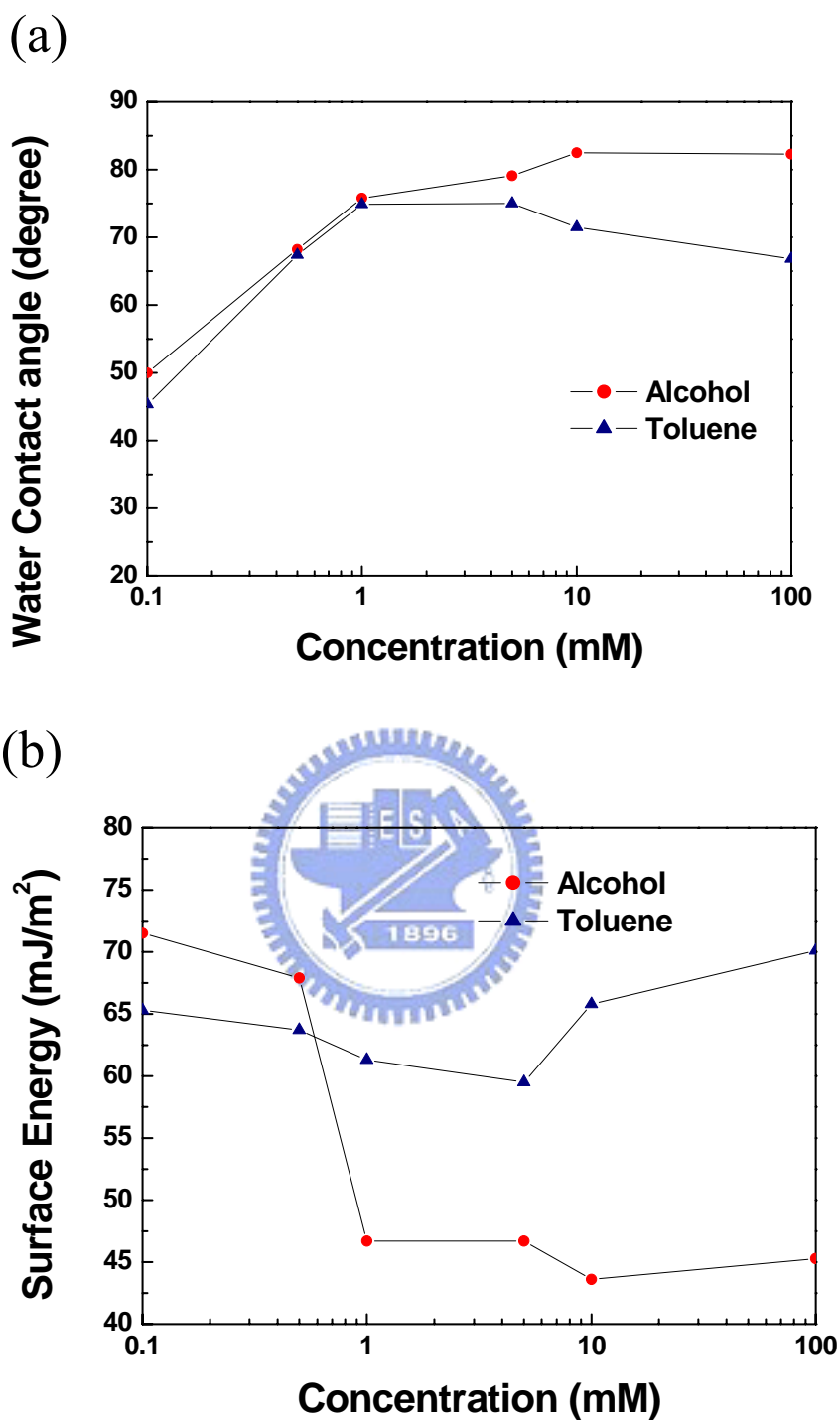
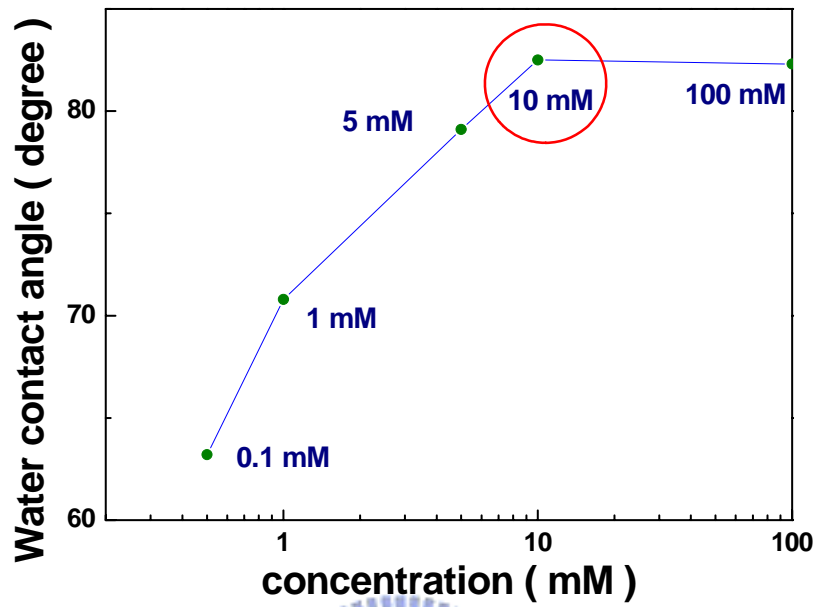


Fig. 3.2 (a) The water contact angle and (b) the surface energy as a function of ODMS concentration. Solvents as alcohol and toluene are compared.

(a)



(b)

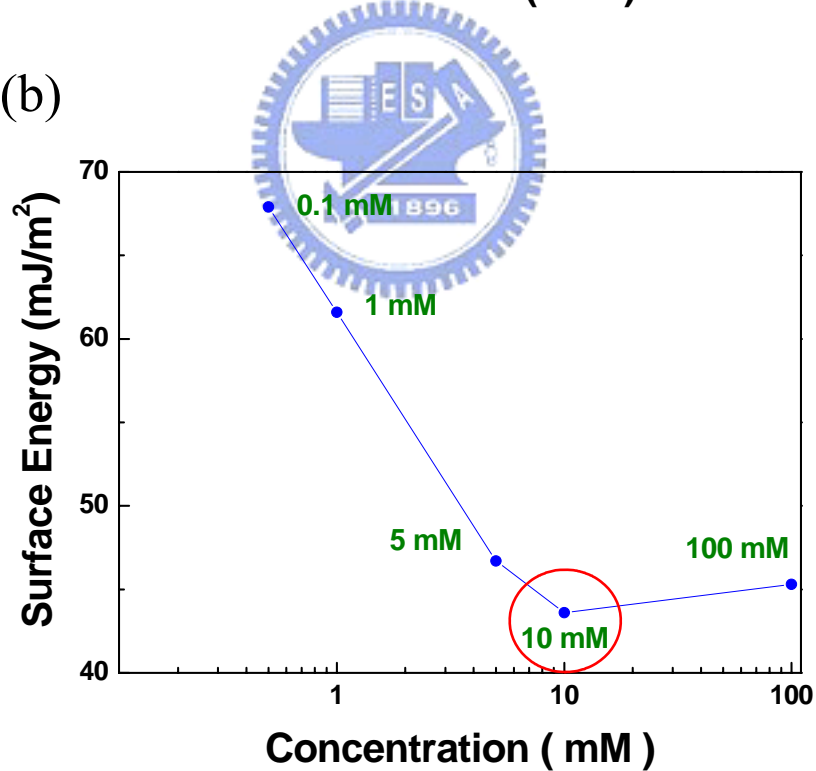


Fig. 3.3 (a) Contact angle and (b) surface energy of SiO₂ treated by different concentrations of ODMS .Alcohol was used as solvent.

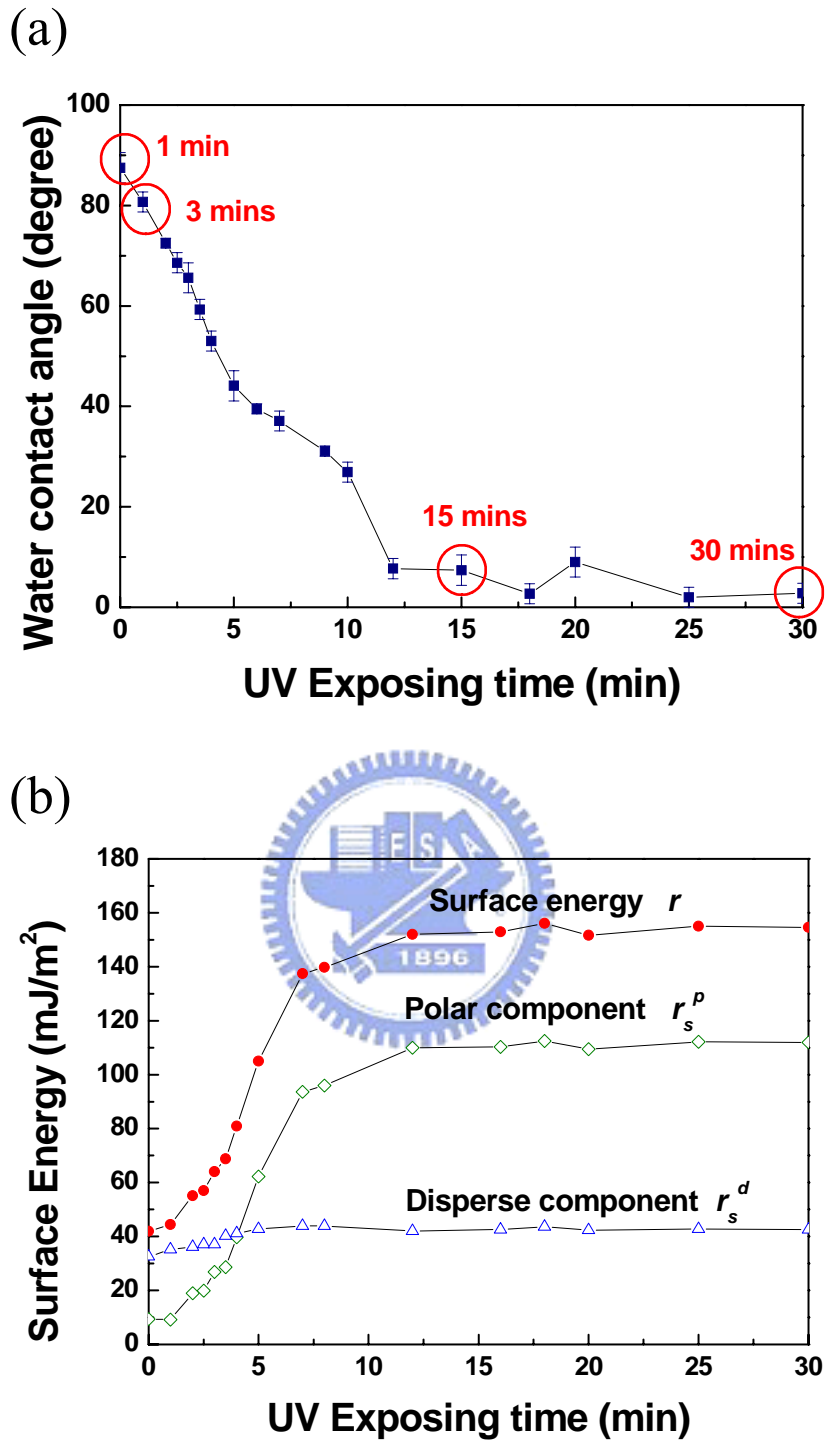


Fig. 3.4 (a) The water contact angle on ODMS-treated SiO₂ surface as a function of UV exposure time. (b) The extracted surface energy and its polar and dispersion components were shown as a function of UV exposure time.

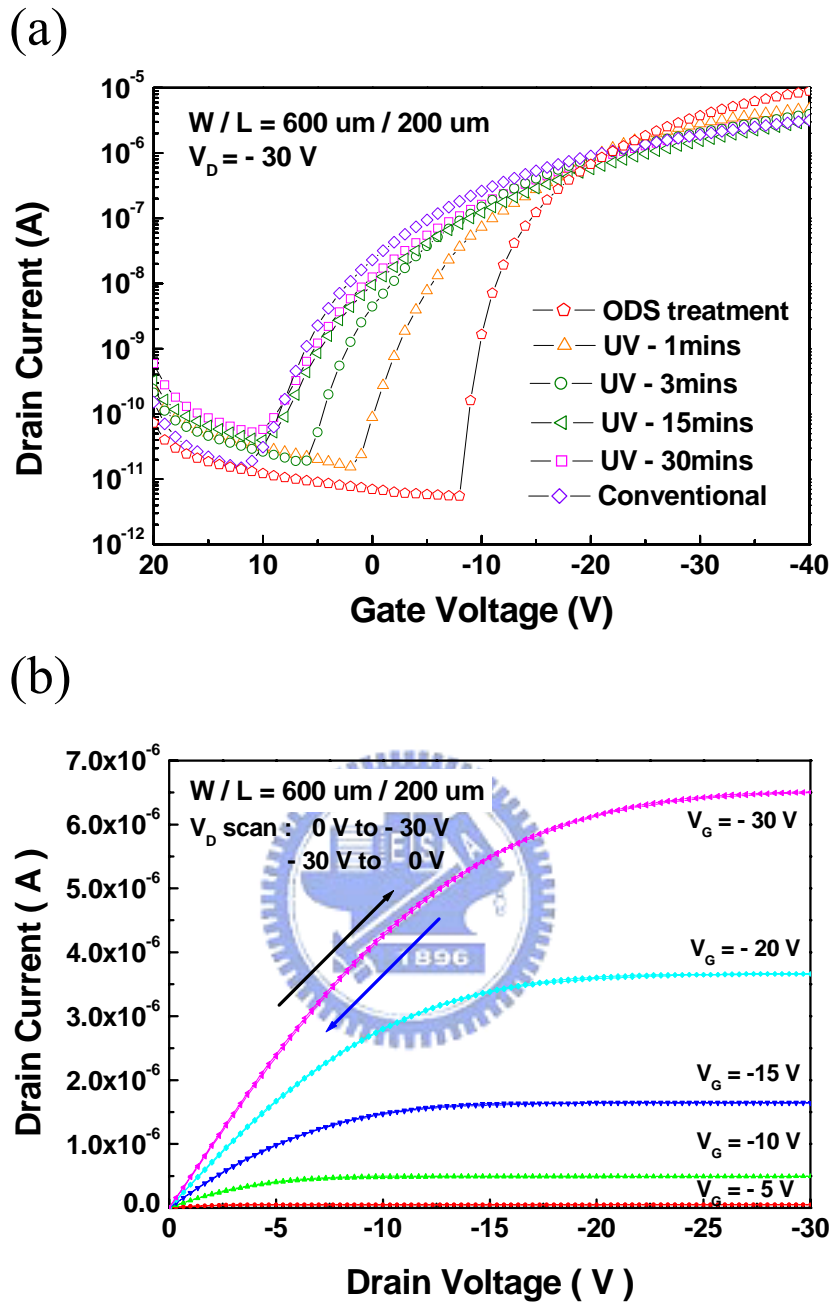
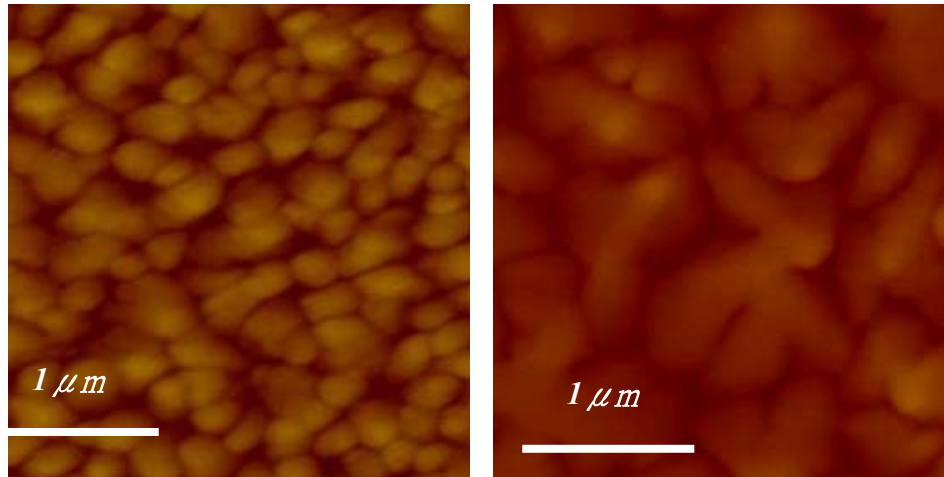


Fig. 3.5 (a) The transfer $I_D - V_G$ curves of various OTFTs with conditions described in Fig. 2.3 (b) The output $I_D - V_D$ curves of ODMS treatment device.

(a)

None UV-exposed

UV-exposed



(b)

None UV-exposed

UV-exposed

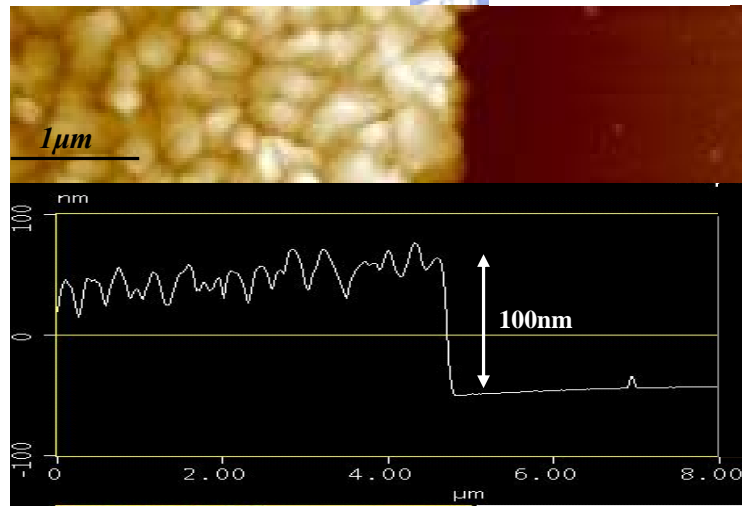


Fig. 3.6 (a) The AFM images of the pentacene deposited on non-UV-exposed region and on 30-mins UV-exposed region. (b) The AFM image and the step profile of patterned pentacene film.

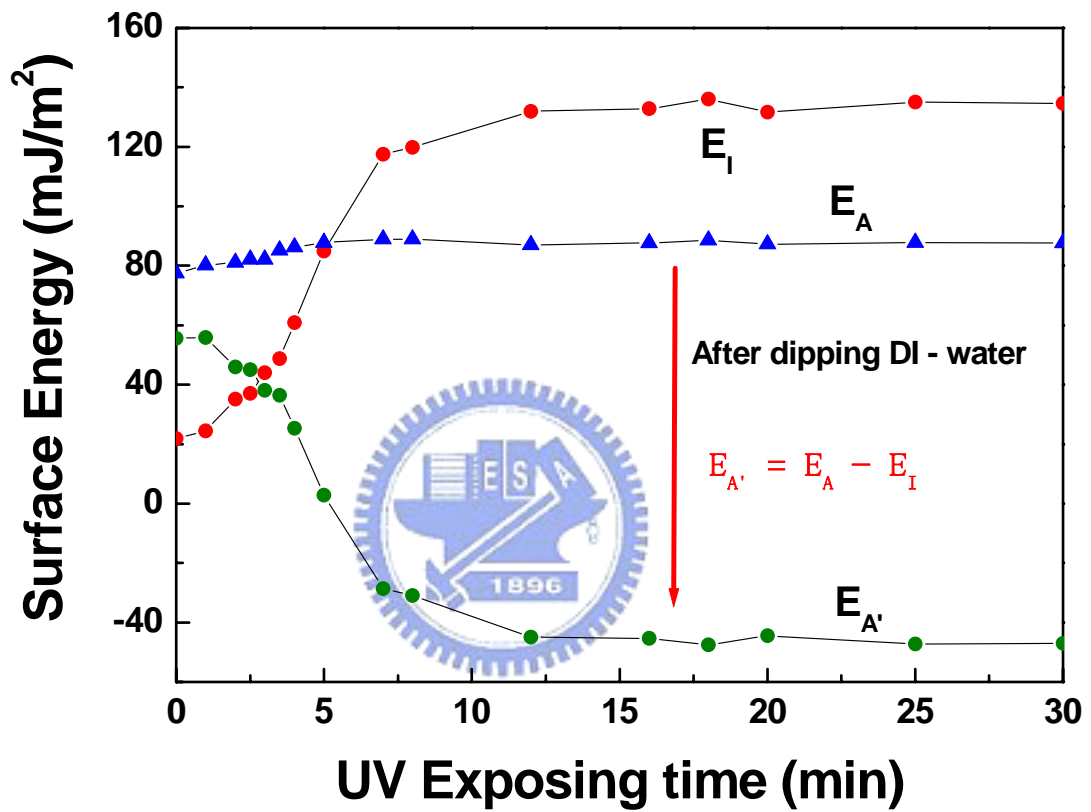


Fig. 3.7 The variation of E_A (adhesion energy before dipping), E_I (intrusion energy), and $E_{A'}$ (adhesion energy after dipping) as a function of UV exposure time.

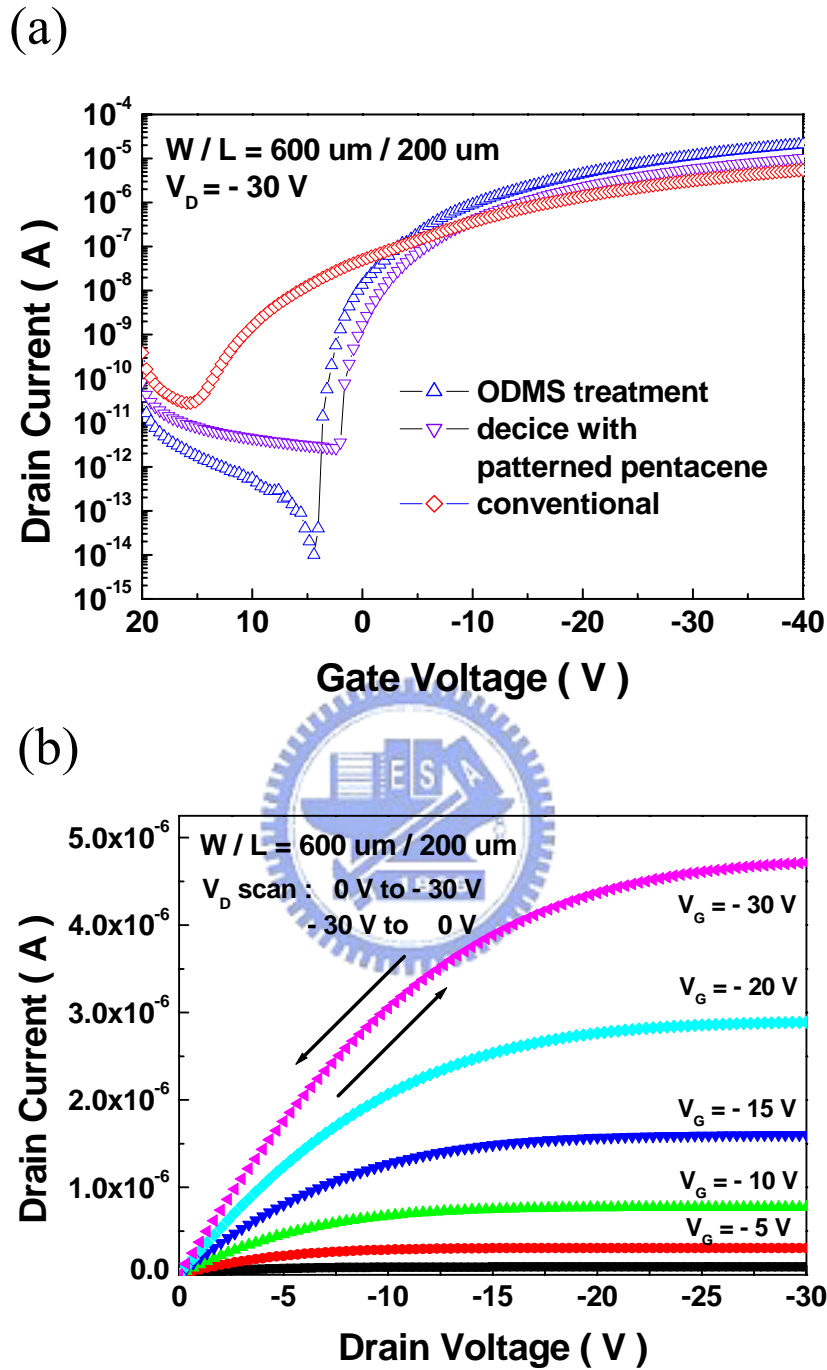


Fig. 3.8 (a) The transfer $I_D - V_G$ curves of various OTFTs with conditions described in Table IV. (b) The output $I_D - V_D$ curves of OTFTs with patterned pentacene.

簡歷

邱育敏

台灣 桃園

E-mail:danielmail.iod93g@nctu.edu.tw

學歷：

國立高雄師範大學物理系應用電子組

(2002.09~2005.01)

國立交通大學電機學院光電顯示科技產業研發碩士

(2005.02~2007.01)



論文題目：

**Pentacene patterning by the adjustment of surface energy
and its application in OTFTs**

表面能調整於定義有機薄膜電晶體主動層區域之應用